Modelling Neural Maturation of the Primary Motor Cortex During Adolescence

M.Sc. Thesis

by

Francis Jeanson
64864

under the guidance of

Dr. Luc Berthouze

Evolutionary and Adaptive Systems
University of Sussex
September 2008

13,129 words

Abstract

The present work introduces innovative results in the domain of neural developmental modeling via computer simulation. In particular, it focusses on the critical developmental aspects of cortical neural activity for motor control. In the introduction, I begin by presenting the scientific context which motivates the work herein. I then introduce fundamentals of neural anatomy for motor control. This is complemented by a formal description of biological neural cells on which the experimental work will be based. Critical aspects of neural activity is then developed. This emphasizes the potentially crucial role played by oscillatory activity in the nervous system. The critical impact of maturation of the brain during adolescence is then explained and taken as basis for the validation of the experimental work. The following chapter presents experimental work on the simulation of a realistic spiking neuron model of the primary motor cortex (Pauluis et al. 1999). Emergent oscillatory activity is obtained and provides the basis for a developmental model of oscillatory dynamics. Various modelling schemes and simulation results of these developmental principles are presented in chapter 3. Although no strong evidence for increasing coherent activity is obtained, some results suggests that a subtle increase may take place when the number of excitatory and inhibitory neurons is reduced. These results are discussed in the end.

Acknowledgements

I would like to thank my supervisor Dr. Luc Berthouze for his helpful advice, encouragement and availability during challenging times. I am grateful to my EASy M.Sc. colleagues for their inspiration, friendship and for making this experience a thrilling one. I am particularly grateful to my parents Patrick and Michèle who have supported me both mentally and financially to accomplish this work. Finally, I would like to thank Ginnie Chen who has continuously encouraged me from the beginning until the end of this degree, and without whom all this would not have been possible.

Contents

List of Figures

Chapter 1

Introduction

1.1 Scientific Motivation

The nervous system is amongst the most complex structural and functional entity known to us. With more than 10^{11} neurons, the human nervous system forms a complex interconnected mesh of neural cells that harbour sophisticated chemical and electrical synergies. Crucially, this mesh changes in structure and function as the individual develops during its lifetime. This continuous development takes place at multiple levels and traverses a multitude of critical stages. Hence, taken together, the nervous system accomplishes the most crucial tasks of complex living organisms: visceral control, sensation, behaviour and thought. Classically, however, these tasks have been perceived as the result of mechanisms which give rise to clear and distinct sets of rules (Haugeland 1985). The brain itself, in the least radical version of this view, is believed to operate in accordance to well defined guide lines. In accordance with this view, it is important to acknowledges the fact that what we seek in an explanation of human sensation, behaviour, and thought is precisely well defined and distinct mechanisms. We should be careful however not to overextend the classically abstract notion of rules with that of real physical mechanisms. The main reason for this stems from the incredible complexity in which living cognition occurs. More recently, investigations in the realm of complexity theory and general dynamics are forging a path towards a deeper understanding of phenomena that appear to be more than what they are made of. The acknowledgement that emergent events are identifiable and quantifiable phenomena constituted by the complex outcome of their interacting constitutive parts has slowly made its way since the mid 1800s into contemporary scientific views (Lewes 1875, Bedau 1997). In parallel, the increasing use of dynamical systems theory for the complex analysis of cognition and behaviour serves as a powerful framework for the proper description and understanding of time dependent phenomena (Kelso 1995). With this approach, it becomes possible to carefully investigate the ways in which a system's variables fluctuate over time, and therefor highlight the initial and sufficient conditions under which emergent phenomena will arise. Furthermore, an eliminative materialism with respect to the function of the mind such as Churchland's, suggests that we investigate the biological and neurological foundation of behaviour, sensation and thought (Churchland 1986). The hope, is that a comprehensive aggregation of neuro-biological and physiological models and data will provide for an unprecedented understanding of complex adaptive behaviour. Here, I intend to make a pragmatic contribution to the study of emergent dynamics at the neuro-biological level by investigating conditions under which oscillatory states

may arise. I also aim in the present work to motivate the claim that a proper understanding of the functioning of complex biological organisms can only be achieved if we situate the processes involved in sensation, behaviour and thought within a developmental time-line. For the nervous system, this can be motivated by significant neuro-imaging findings which show that the brain continues to develop from childhood to mature adult age (Gogtay et al. 2004).

To accomplish this, I begin by introducing some fundamental aspects of the structure of the nervous system with a particular emphasis on motor control. Following this, some biological and formal descriptions of neural functioning is developed. I then motivate a particular interest with respect to a potentially significant form of information coding via oscillations, and finally introduce fundamental aspects of development in the nervous system during adolescence. With this foundation in mind, a novel model of developmental neural group dynamics for the primary motor cortex is proposed but also tested via simulation and analysis.

1.2 Motor Control

Why should we be interested in motor control? A fundamental aspect of agent adaptation stems from the ability to move a body in space. The modern definition of life is known as autopoiesis (Maturana and Varela 1980). It requires that an organism actively maintains its internal structure to stay alive - also known as *organisational closure*. This definition however does not require that the motion of an agent is important, but abstracts from the fact that environmental conditions of the agent aren't necessarily consistent. Although organisational closure is fundamental to life, there can be clear advantages in becoming mobile. An obvious case would come as the act of foraging for food at a new location when resources have become scarce in the local area. Ross Ashby formalised the foundation for this increase in adaptive ability by highlighting the notion that an agent can only cope with fluctuations in the environment by generating fluctuations of its own to counter them. In his words: "variety can destroy variety", which he denotes as the law of *Requisite Variety* (Ashby 1956 p. 207). With respect to agents however, we can distinguish between two categories of variety: internal or external. Internal variations can be regulated by internal mechanisms, such as the part played by the liver to regulate changes in sugar concentration in the blood stream. Arguably internal variation fulfills the most fundamental form of regulation by maintaining all visceral functions of the body in proper order. External variation takes place when the mechanisms of internal variation are insufficient to cope with important fluctuations. This external variation manifests as motion in space of the entire body or of some appendages (e.g. arms and legs). By doing so, the agent can extend its regulatory ability considerably. In fact it appears reasonable to claim that developing the ability for external variation (i.e. movement) in combination with sensation is the precursor to the evolution of a complex nervous system.

The human nervous system spans across the entire body from head to toe forming a complex network of neural cells and corresponding axons which radiate from the brain and the spinal cord. Neurons which transmit signals form the brain and spinal cord to the body are denoted *efferent* neurons, whereas those which transmit information form the senses back to the spinal cord and brain are named *afferent* neurons. The brain lies at the top of the spinal cord and is constituted by a highly dense structure of neurons, support cells and tissue. Although the brain

is clearly segmented in a number of general parts such as the medulla omblogada, the pons, the cerebellum, the midbrain and the diencephalon; the neocortex which lies on the exterior of the brain is responsible for the complex coordination of sensory input, motor control, but also harbours key processes of higher order cognition such a thinking and reasoning.

Motor control is achieved in humans by the complex activity of four cooperative motor systems (Purves et al. 2001, p. 384). The primary motor system is constituted of the spinal cord and its related efferent and afferent neurons. Skeletal muscles are innervated by the efferent α and γ motor neurons which originate from the spinal cord or the brain stem. α motor neurons command the contraction of extrafusal muscle fibers whereas γ motor neurons regulate the afferent signal by contracting the intrafusal muscle spindle. The signal of these motor neurons originates from the spinal cord. Although signals to the spinal cord often arrive from the brain, local circuits of neurons within the spinal cord serve the purpose of basic reflexive movement. For instance Renshaw cells recursively inhibit the motor neuron that causes itself and the muscle fiber to excite (Baldissera et al. 1981). Reciprocal interaction is another form of spinal local circuitry (McMahon 1984). Here for example, the afferent signal coming from the flexor of a limb to the spine may inhibit the activation of motor neurons of the limb's extensor. In fact as demonstrated by the early work of Sherrington, rhythmic contractions of a cat's legs continues to occur after the spinal cord is severed from the brain (Sherrington 1906). More recent findings by Cohen, Rossignol and Grillner demonstrated that completely isolated spinal circuits in the ventral root still gave rise to rhythmic bursts (Cohen et al. 1988). These findings lead to the acknowledgment that central pattern generators situated in the spinal cord are sufficient to account for the basis of locomotion.

The secondary motor system includes the descending motor components which directly stimulate the local circuits of the spinal cord or muscles. These are the brainstem and the motor cortex. The brainstem, which lies at the top of the spinal cord, plays the part of an important signal generator responsible for balance, posture, but also basic orientation of the eyes, head and body with respect to sensory information. It accomplishes this orientation via input from the coordinative processed that take place in the cerebellum, known as the third motor system. The cerebellum is situated at the back of the brain and projects signals via the cerebellar peduncles to other motor areas of the brain. It contains a highly dense network of neural cells which comprises more than half of the total number of neurons in the brain (Ito 1984). The primary roles of the cerebellum are to regulate muscle tone, coordination of movement with respect to sensory stimuli, timing of movements, and motor learning (Rosenbaum 1991, p. 52-56). The cerebellum in fact works as a regulating system for all high level motor control processes and does so by directly or indirectly modulating upper motor neurons in the motor cortex and the brainstem.

The fourth motor system involves the roles played by the basal ganglia. This system of nuclei is located within the central regions of the brain. These nuclei include the putamen, the caudate, the globus pallidus, the subthalamic nuclei, and the substantia nigra. Similar to the cerebellum its role is to regulate the activity of upper motor neural activity in the motor cortex primarily. Upon input from the cortical areas, the caudate and putamen propagate inhibitory signals to the globus pallidus and substantia nigra. The globus pallidus then sends inhibitory signals to the motor cortical areas via the thalamus, while signals emanating from the substantia nigra inhibit activity in the superior colliculus controlling head and eye movement (Purves et al.

2001, p. 391). Hence the basal ganglia serves principally as an inhibitive system. The thalamic inhibitions that originate from the globus pallidus in fact serve to disinhibit the thalamic neurons which control upper motor neurons in the neocortex. Disruptions to these mechanisms explain conditions such as Huntington's disease and Parkinson's disease. Behaviourally then, the basal ganglia plays a key role in the initiation or retrieval of movement plans (Marsden 1982).

Part of the secondary motor system, the motor cortex occupies three particular regions of the frontal lobe: the primary motor cortex, the lateral premotor cortex, and the medial premotor cortex. These regions are generally responsible for the planning, initiation and direction of temporal motor sequences. This system is thus the source of complex motor actions that go beyond the reflexive. By 1870 the physiologists Theodor Fritsch and Eduard Hitzig confirmed the notion that some spatially distributed cortical areas are responsible for various muscles of the body. They had in fact discovered the primary motor cortex (MI) in a dog's brain by directly stimulating areas of MI with electrodes and observing immediate muscle contractions. This topological relationship between various regions of MI and muscles throughout the body in humans was confirmed by Penfield and Rasmussen with their work on epileptic patients (Penfield & Rasmussen 1950). They derived from these experiments the well known *motor map*. The corticospinal tract, i.e. the pathway that axons borrow to reach the spine from the cortical neurons, has since been accurately identified (Purves et al. 2001, p.376). Experimental recordings from MI and muscle neuron of the index finger showed that a 50ms delay occurs between the activation in MI and the onset of finger motion (Deecke et al. 1969). This short delay suggests that MI is amongst the final sites of neural activity before muscle neurons are triggered. Hence MI can be considered as a triggering centre for motor action. Beyond simple notor neuron triggering, MI also appears to encode for the application of force and direction in movements (Evarts 1981, Georgopoulos et al. 1986). The primary motor cortex also establishes significant reciprocal connections with the premotor cortex. This area transmits signals from other regions of the cortex to either the primary motor cortex or directly to the lower motor neurons. The lateral premotor cortex however plays an important role in the learning of coordinated motor control with visual or temporal cues.

As mentioned above the importance of motor control for intelligent adaptive behaviour is fundamental. Although this overview of the regions responsible for motor control indicates the overall areas involved in behavioural action, it does not provide any insight into the nature of the neural mechanisms that give rise to these actions. To better understand these mechanisms it thus becomes relevant to explore the dynamics of individual cells involved in motor action and their cooperative effects as a whole. Because the project of detailing all nervous regions involved in motor control is too vast, the focus of this report is to explore these mechanisms with respect to the brain area directly responsible for muscle control: the primary motor cortex.

1.3 Cortical Motor Neurons

By the end of the 19th century Ramón y Cajal, using Golgi's staining technique, observed that the nervous system did not form a continuous reticular structure but that it was constituted by clearly individuated cells. By doing so he established the neuron doctrine: the notion that each neural cell corresponds to an individual functional unit of the nervous system (1909). All

neurons have the unique ability to transmit an electric current across their axon in order to signal other neurons. Furthermore, the signal received by neurons is made on average by up to 10^4 synaptic connections (Rosenbaum 1991). Although all known neurons in the brain function by the same base electrical principles, the diversity of neurons in size, shape and function is large. In the motor cortex three main neuron cells can be found: the stellate cells, the pyramidal cells, and fusiform cells. These neurons are organised into six layers of the cortex over a total thickness of about 3-6mm. The molecular layer (layer I) is located at the surface of the cortex, while the granular layer (layer II), the pyramidal layer (layer III), the inner granular layer (layer IV), the inner pyramidal layer (layer V), and the fusiform layer (layer VI) lie below. Stellate and pyramidal cells are found within each of these layers, although their size may increase in deeper layers. There are however no sharp organizational demarcations between these layers In the primary motor cortex special pyramidal cells (Betz cells) located in layer V propagate signals from the cortex directly to the brainstem and spinal cord. These cells are responsible for the final motor signals (Purves et al. 2001, p.376). Total density of neural cells in the motor cortex of humans is of about 30,000 cells per cubic millimeter, with significant variation between layers (Blinkov & Glezer 1968). Also, the proportion of these cells varies with respect to type and function. Pyramidal cells in the prefrontal cortex have been estimated to constitute about 72% of the total neural population whereas 26% for stellates and 2% for fusiform cells. Furthermore, in the neocortex, an estimated 85-90% of these cells are excitatory versus 10-15% inhibitory (Abeles 1991, p.50-53).

Indeed the fact that neurons can stimulate post synaptic targets in an inhibitory or excitatory fashion constitutes a fundamental aspect of neural functioning. It is important to note however that the excitatory or inhibitory effect is not only determined by the signaling neuron but also by the membranous properties of the target neuron and whether it posses the appropriate receptors for the incoming synaptic neurotransmitters (Kandel et al. 2000). Neural activity is characterised by the combined action of electrical potentiation and chemical transfer. Neurons generate electrical action potentials in order to trigger synaptic signal transmission. This action potential is initiated by a change in cytoplasmic ion concentration which is then transfered via the cell's axon to the terminal synapses which terminate either at a dendrite or the soma of a target neuron. Three ions are commonly involved in neural activity: potassium (K^+), sodium (Na^+), and calcium (Ca^+). At rest, neurons actively maintain an uneven electrical balance between their inner membrane space and the environment by maintaining via ion gates and K^+ pumps a higher amount of K^+ within the cell than outside. This ensures that a negative (e.g. -50mV) but equilibrated state is maintained. The advent of a synaptic discharge[1] causes neurotransmitters to bind to Na^+ ion gates situated on the membrane of the neuron. This allows high concentrations of external Na^+ to penetrate the cell therefor increasing the positive charge within the cell which then depolarizes the membrane. If this depolarization is sufficient to elicit further opening of Na^+ ion gates then a positive feedback engenders a significant depolarizations. If this depolarization reaches the membrane's electrical threshold an action potential is triggered and propagated in turn to the axon. By behaving in such an 'all or nothing' manner we say the neuron spikes or emits a pulse. The gating of ionized molecules by the membrane can be interpreted as membrane conductance, i.e. the amount of charges that traverse the membrane with respect

[1]Less common electrical transmission via gap-junction are also found in various areas of the brain.

to the difference of potential between the inside and outside of the cell. By doing so Hodgkin and Huxley were able to determine a mathematical formalisation that can adequately relate the amount of current flowing through the membrane with its conductance, resting potential, and current potentiation (Hodgkin & Huxley 1952). This gave rise to the following equation,

$$I_o = g_o(V_m - E_o) \tag{1.1}$$

where I_o is the amount of ionic current flowing through the membrane for ion o (in Amps), g_o is the conductance of the membrane for ion o (in Siemens), V_m is the current potentiation of the membrane (in Volts), and E_o the equilibrium potential for ion o of the cell (in Volts).

How do we get excitatory signaling from this relation? If we consider an artificial neural cell that possesses a single type of ion gate, say o^+, and no other ions are present in the environment, we can determine the current flowing through the membrane with respect to the amount of ions the gates permeate. If o^+ is found in larger concentration on the outside of the cell then $V_m < 0$. If the ion gates are open (i.e. $g_o > 0$) then there will be a diffusion of o^+ towards the inside ($out \rightarrow in$). Because o^+ is positively charged this increases the charge inside the cell, hence increasing the membrane potential. This influx of ion in the cell membrane will continue until the equilibrium potential E_o is reached, or in other words until $V_m = E_o$, i.e. depolarization. Thus if in the initial condition $E_o > V_m$ and the ion gates are open there will be excitation of the cell. These conditions essentially describe the principles behind Na^+ ion fluctuations. To generate an inhibitory signal it then suffices to set an initial condition where $E_o < V_m$. If the cell at equilibrium is already polarized to a negative value (i.e. $V_m < 0$) and a large concentration of ions are inside the cell but less than charges outside then the opening of ion gates (i.e. setting $g_o > 0$) will provoke a flow of ions from the inside to the outside of the cell ($in \rightarrow out$). This causes further differentiation which then hyperpolarizes the cell membrane.

By using this interpretation, it then becomes possible to abstract from the complex dynamics of chemical flow by describing changes of a neuron's signaling properties purely in terms of potentiation, ion specific rest, and ion specific conductive change. This formulation will be used in the experimental conditions of the following chapter. This principle isn't sufficient however to understand the immense operational capacity of the nervous system such as the ability to feel, to think, and to behave.

Ultimately our goal is to identify the fundamental principles of neural dynamics as a cooperative whole and see how they allow complex organisms to adapt to their environment. Over the past century, models of neural mechanisms have refined their understanding and proposed new and potentially significant principles. Amongst the first, the principle of threshold neuron suggested by McCulloch and Pitts in the early 40's, has had a tremendous influence in the field of theoretical neuroscience and artificial intelligence (McCulloch & Pitts 1943). This mechanism, which is meant to describe the 'all or nothing' behaviour of neuron action potentials, has given rise to the modern field of artificial neural networks (Rumelhart & McClelland 1986, Churchland & Sejnowski 1992). In their view an activation function must determine whether the incoming signals to the cell are sufficient to cause the cell to ouput a signal of its own. This approach however has based the performance of real biological nervous systems on the conception that neural firing rate is the key informational mechanism that gives rise to complex behaviour. Indeed, the activation function in such architectures provides a real valued signal at each output neuron.

This value is meant to encode the normalized firing rate of realistic neurons over a period of time (Vreeken 2003). Although the rate coding principle does indeed seem to bare significance to the functional operation of nervous systems, some biological evidence has challenged the idea of rate coding as the only relevant mechanism. Some findings for instance have shown that humans classify visual information for facial recognition in less than 100ms (Thorpe & Imbert 1989). Yet at least 10 neural layers are required for transmission from the eye to the visual area, leaving only about 10ms for neurons to process the incoming signal at each stage. Furthermore cortical firing rates rarely go beyond 100 spikes per second, thus leaving no time for significant rate coding to occur. Instead it has been argued that neurons must use spatial and temporal aspects of incoming signals to generate spikes (Perkel & Bullock 1968, Thorpe et al. 2001). This can be generally referred to as spike coding. Although a number of plausible mechanisms have been proposed, one particular approach is gaining increasing interest due to both its pervasiveness in the nervous system and its fidelity to a core characteristic of the brain: the actions of neurons en mass. This view regards synchronized activity of neurons via oscillatory firing as a potentially crucial principle in neural information processing.

1.4 Oscillatory activity in the Primary Motor Cortex

Rhythmic activity in the nervous system has been first been identified in the 1930's by Hans Berger (Buser & Rougeul-Buser 1995). Typically however, these rhythms have solely been considered as pure epiphenomenal indicators of cognitive status without functional purpose. Four typical frequency bands have been identified and correlated to various cognitive states. Slow frequency delta waves (1-4Hz) are recorded during the sleeping state. Spindle oscillations, or alpha waves (7-14Hz) are also commonly found in early stages of sleep, between sleep phases, or wakefulness. Whereas, beta (15-29Hz) and gamma (30-80Hz) frequencies are predominant during attentive waken activity (Bazhenov & Timofeev 2006). Since the 1980's a gaining interest in the potential that synchronized oscillatory activity may play a role in cognition has given rise to a number of hypotheses and experimental testing.

The activity of neurons in the different regions of the brain triggers location specific oscillations, but before investigating the functional possibilities of such activity it is crucial to identify its origin. Until the mid 90's the dominant view has been to see oscillations in the brain as originating from the thalamus and projected to various parts of the cortex (Steriade et al. 1990). Amongst the strongest supporting evidence for this claim comes from Morison & Bassett who recorded oscillations from the thalamus of cats with the cortex removed (Morison & Bassett 1945). More recent studies have shown that the various rhythms exhibited by the cortex are typically accompanied by activity in thalamic nuclei (Buser & Rougeul-Buser 1995). To explain the origin of oscillations in the thalamus, a few hypotheses have been tested. The first states that cells in the thalamus intrinsically oscillate, which has been observed with in-vitro experiments. Alternatively, because relay cells in the ventralis posterior nuclei (VP) don't oscillate in response to cortical stimuli, one hypothesis claims that two types of cells exist in these nuclei: relay cells and rhythmic cells; or alternatively that they transfer between oscillating and relay modes (Janhsen & Llinas 1984). The third most probable hypothesis was emitted by Steriade & Deschenes: that only the nucleus reticularis of the thalamus (RET) is responsible for oscillations,

and that via its recurrent connections to other thalamic nuclei it induces thalamic and subsequent cortical rhythms via projections to it (Steriade & Deschenes 1984). Interestingly further experimentation by Buser & Rougeul-Buser have also observed that RET plays a role for spindle oscillations but not for the higher beta or gamma ranges. However, recurrent connections are not enough to explain the emergence of RET oscillations, but because the neurons of the reticulum are primarily GABAergic they would constitute a feedback loop of inhibitory connections. It is then argued that this construct would be sufficient for the appearance of oscillatory activity in the RET.

Is is important to realise that taken together, these perspectives fail to consider the possibility that oscillations in the cortex may arise on their own without rhythmic stimulation from thalamic nuclei. Although initially unpopular for the evidence suggested above, this view is progressively gaining ground. Analytical work on the dynamical properties of coupled neurons by Wilson and Cowan in the early 70's was probably the first to introduce the possibility that a heterogeneous network of randomly connected inhibitory and excitatory cells can give rise to oscillatory states (Wilson & Cowan 1972). Twenty years later, this work began to gain biological support. In 1990, Steriade et al. conducted experiments showing that a variety of pyramidal neurons could give rise to oscillatory activity on their own in-vitro given the right chemical environment (Steriade et al. 1990). The artificiality of the experimental setup cast doubts however onto the claim that just about any neural structure in the brain could potentially trigger rhythmic activity. In 1991 however, Engel and colleagues illustrated that interhemispheric coherence could not be sustained after sectioning fibers of the corpus callosum of the cat (Engel et al. 1991b), thus suggesting that cortico-cortico connections may be necessary if not sufficient for some synchronized activity in the brain. With respect to motor control, Murthy and Fetz in 1992, are probably amongst the first to observe and acknowledge that beta and gamma frequencies may emerge in the sensorimotor cortex of monkeys due to motor and sensing coordination (Murthy & Fetz 1992). By recording the local field potentials (LFP) of the somatosensory and somatomotor areas of the cortex, they detected strong oscillations in the 25-35Hz range when monkeys had to search via tactile exploration for raisins placed in a container located outside of their visual field. Because their recordings consisted of local field potentials these results also suggest that significant synchronization between neurons occurred. They noticed that while oscillations appeared in the reward search task, no oscillations took place during well trained automatic movement. Neither where these oscillations closely correlated to specific motor behaviour. According to them however, they should play an important role for the recruitment of post-synaptic targets, which is facilitated by synchronous firing. Furthermore they noticed that synchronized activity remained local with a significant decrease in coherence beyond distances greater than 14mm. Although their results are not sufficient to rule out the possibility that extrinsic activity from areas such as the thalamus may play a role in the oscillatory activity of the somatosensory and somatomotor areas, the implication of sensory motor coordination as a driving mechanism for coherent oscillations in these experiments suggests that their origin could be more tightly coupled to their local function than to some extrinsic control mechanisms. More recent evidence for the emergence of oscillations in localized neural structures comes from computer simulated modelling.

With the significant increase in computer power it has become possible to model and observe the behaviour of relatively large neural populations (Wang et al. 1995, Bush & Sejnowski 1996,

Pauluis et al. 1999). The motivation behind this approach, is two folds: to asses whether the current neuro-physiological knowledge of neural cell dynamics and interaction is sufficient to explain cognitive phenomena, and if so, to make predictions about such phenomena via simulation and complement our current knowledge. Bush and Sejnowski in particular, successfully modelled the emergence of oscillations and the coherence between a small number of biologically realistic neurons within a single population of layer V, but also between two cortical column populations (Bush & Sejnowski 1996). Inspired by this work Pauluis et al. designed a much larger network of 10,000 neurons which also displayed oscillatory emergent properties (Pauluis et al. 1999). These results were only attainable by following what Wilson and Cowan had originally stipulated: that the presence of excitatory neurons alone is not enough, but that a percentage of inhibitory neurons within a population of excitatory neurons is sufficient to exhibit the emergence of rhythmic activity. What I haven't yet motivated however, is why coherent oscillations may at all be important for cognitive tasks.

As mentioned above, Murthy and Fetz suggest that synchronous firing should promote the recruitment of new targets more effectively (Murthy & Fetz 1992). The monkeys exhibited such firing patterns especially during sensorimotor coordinated tasks. It may be possible then that rhythmic firing could give rise to task specific 'channels' between cortico-cortico pathways but also between the cortex and the rest of the brain. Beyond recruitment however, it seems possible that synchronous activity could also play a fundamental role in context dependent information coding. For example, evidence from visual perception studies have suggested that coherent nerve cell firing could be responsible for effective visual feature detection (Eckhorn et al. 1988, Engel et al. 1991a, Freiwald et al. 1995, Kreiter & Singer 1996, Taylor et al. 2005) . Eckhorn et al. found significant gamma range oscillatory activity in the visual cortex of rats which were presented with visual stimuli. They propose that oscillatory activity in the visual cortex may serve as a second level coding scheme for the linking of similar features and act as temporal labels to bind features into a single perceptual entity (Eckhorn et al. 1988). An early attempt to interpret the mechanisms in which the brain could determine the features of a visual scene has led to the claim that a one to one feature to cell mapping takes place (Barlow 1972, Engel et al. 1991a). Engel and colleagues, as others, warn however that such a mapping would result in a combinatorial explosion: the number of potential features in a visual scene could potentially be limitless especially as new objects are presented. This would result in the incapacity for the subject to recognize or learn about any new object after a certain point, which clearly does not occur. Instead they propose that phase locking of oscillating neural firing could allow such feature detection. Thus by temporally coding edge detecting neurons, segments of a visual scene can be recognized. This spatiotemporal coding scheme via synchronized oscillatory activity of neuron groups may thus constitute a crucial process which the nervous system takes advantage of for a particular set of sensorimotor but perhaps also higher cognitive tasks.

It would be obtuse however to consider the nervous system as a highly complex but overall cyclically stable system. In reality it is a highly malleable and plastic entity which continuously changes in function and structure over various time scales. Electrical activity of the neurons for sensing, control, and decision making occurs probably at the shortest of these time scales. Learning via synaptic plasticity undoubtedly occurs over a longer period. But it is also important to consider how deeper structural changes take place over the life time of the insect, animal, or

individual. By better understanding the manner in which the nervous system physiologically and functionally progresses over longer time scales should allow for an accurate understanding of how adult behaviour and intelligence comes in place. Development in a sense, sets cognitive capabilities into context. In the following I care to motivate the importance of maturation of the nervous system during critical stages of life.

1.5 Maturation of the Nervous System

It is easy to attribute behaviours as being part of the brain, but in reality they are the product of a tight coupling between environment, body, and cognitive mechanisms. Similarly we must pay attention not to overextend this fallacy and claim that behaviours are in the genes. The contemporary enthusiasm for genetic research as the science than can "heal all ills" can easily dupe the uninformed. Genetic regulation is fundamental to life and intelligent behaviour, yet the mechanisms involved in this regulation remain local and fully determined by their environmental conditions. Hence it is crucial that we do not underestimate the impact of epigenetic mechanisms during the individual's life, and the potential impact it may have on any sensory, motor and cognitive abilities. Although highly reliable, the mechanisms involved in the development of the nervous system occur over various critical periods: from the beginnings of gastrulation of the embryo, to neurulation in the womb, then postnatal nerve development, and continued myelination during life. In the current context I will focus on the aspect of neural development from adolescence until young adulthood.

By the early 1980's, studies on the effects of age on the nervous system originated primarily from post-mortem studies of individual brains at different stages of puberty (Blakemore & Choudhury 2006). In these studies it was noticed that two important factors changed in the cortex during adolescence : increase in myelination, and synaptic specialization (Yakovlev & Lecours 1967, Huttenlocher et al. 1983). Myelination is a process by which special macro-glial cells wrap around neural axons at regular intervals to facilitate electrical transmission of action potentials. This process has been detected as an increase in white matter in a continuous fashion as the child ages. Interestingly, this increase continues in the prefrontal and parietal cortex until early adulthood, but in other areas such as the sensorimotor regions this myelination is complete by early childhood (Yakovlev & Lecours 1967) These findings have been corroborated more recently with magnetic resonance imagery (Paus 2005). This increase in myelination appears to significantly contribute to the improvement of reasoning, speech and better communication between cortical and sub-cortical areas. The second important aspect of adolescent neural development comes from histological and modern imaging techniques showing non-linear changes in the amount of gray matter of the cortex (Huttenlocher et al. 1983, Gotgay et al. 2004, Sowell et al. 2004). Recent assessments have shown that the thickness of the gray matter in the cortex has an overall tendency to increase at early ages of infancy followed by a short plateau and a general decrease at the onset of puberty until early adulthood (Gotgay et al. 2004). Unlike axonal myelination of the white matter, change in cortical thickness does not occur linearly over the entire brain. This change in density is primarily attributed to reduction in synaptic density. After significant proliferation of connectivity via synaptogenesis during childhood, competing connectivity appears to drive significant pruning of dendritic and somatic connections from af-

ferent axons in the cortical layers (Bourgeois et al. 1994). In contrast preserved connections are reinforced which are believed to improve the efficacy of cell networks in their functional task. In the prefrontal cortex of the rhesus monkey Bourgeois et al. noticed that the density of neuropil decreased significantly after two moths of age until the age of 20. At 2 months the neuropil density of layer II and III was 84%, but at 20 years the density reduced to 71% for layer II and 66% for layer III. Thus corresponding to a maximum reduction of 21.4% of neural filaments of the gray matter. From their longitudinal neural imaging study, Gotgay et al. found however that a sharper and linear decrease occurs in the motor cortex of humans than in the prefrontal cortex (Gotgay et al. 2004). Although not explicit in their report, there appears to be approximately 82% of neuropil at the age of 5 with a reduction to 48% at 20 years of age in the human motor cortex. Due to a lack in quantitative data on the precise synaptic densities in the various levels of the motor cortex of the human brain, an approximate estimate as to the amount of neuropil loss in the human cortex during development can be averaged to about 34% from the age of 5 to 20. These figures will be useful in the following section on the modelling of neural change during adolescence.

The functional implication of this decrease in synaptic connectivity is poorly understood. Studies on the potential behavioural impact of synaptic pruning and myelination are becoming more common (Sowell et al. 2004, Paus 2005). In general studies which focus on cognitive changes related to age in the young normally developing individual should exhibit some correlation between performance and synaptic or myelination changes. Luciana and Nelson for instance noticed that prefrontal working memory improves significantly between the ages of 5 and 7 (Luciana & Nelson 1998). There is still however quite a poor understanding of the more immediate impact of these cortical changes on the operational role of neural groups and their interactions. Although the impact of synaptic strengthening and pruning undoubtedly plays an important role in increasing the reliability and quality of the information communicated between cortical regions and between the cortex and sub-cortical areas of the nervous system. Oscillatory activity is often not considered however. Although some studies have tracked the effects of puberty on rhythmic activity of the brain, little but existing evidence has shown that maturity may have an impact on oscillatory coherence (Gasser et al. 1988, Marshall et al. 2002, Farmer et al. 2007).

Gasser et al. did inspect the effects of puberty on brain waves (Gasser et al. 1988). By looking at children between the ages of 6 and 17, they noticed that low frequency delta, but also theta, alpha and beta bands tended to diminish in power overall with age. Strong difference with respect to location and wave band were recorded however; as for the cortical area 4 they found that relative spectral band power reduces from 28.5 to 22.8 between the age of 6 and 17 for delta frequencies, from 33.2 to 25.3 for theta frequencies, it remains unchanged for low band alpha (7.5-9.5Hz), increase from 7.2 to 11.4 for high band alpha (9.5-12.5Hz), from 5.2 to 8.3 for low band beta (12.5-17.5Hz), and also increases from 3.4 to 6.0 for high band beta (17.5-25Hz). Hence, as the individual ages, lower frequency components are dampened whereas frequencies above 7.5Hz are amplified in the motor area. Although local field potentials recorded by electroencephalography (EEG) imply that local synchronization takes place in the cortical areas recorded, they don't indicate any potential distal cooperation between different brain regions or between the brain and other parts of the nervous system. By measuring activity between motor cortex and muscle control it may be possible to detect important implications of

synchronized firing in nervous systems. Within the past decade, distal coherence has indeed been observed for motor control (Conway et al. 1995, Farmer et al. 2007). Conway and colleagues conducted the first experiment showing significant synchronization between brain wave activity and voluntary motor contraction. Using magnetic encephalography (MEG) to record cortical activity on either the left or right side of the cortex and electromyography (EMG) to record left and right 1DI muscles of the hands. Their results showed significant coherence in the frequency range 12-31Hz between the dominant hemisphere and the contralateral hand over all subjects when asked to contract the muscle at less than 10% of the maximum voluntary contraction. Outside of this range coherence was not significant. Although this study does not provide any insight as to the developmental timeline of oscillatory synchronous activity, it does indicate a potentially significant functional role played by synergistic effects in the cortex for behavioural control. To study the impact of developmental changes with respect to rhythmic activity more contemporary work had been conducted. By recording motor neuron activity of the short and long thumb abductors using electromyograms (EMG), Farmer et al. sought to detect whether the 20Hz band oscillatory drive from the cortex to the motorneuron pool of the hand changes with age (Farmer et al. 2007). After testing EMG-EMG coherence between both thumb muscles for individuals betweeen the ages of 4 and 35, they detected that the most significant increase in coherence took place in children between the ages of 7 and 14. Because, this increase was most notable in the 20Hz band, these results seemed to confirm that important synaptic activity continues to occur in neural connectivity from the cortico-spinal to motor neurons. As they note, this increase in synchrony could be a major cause for the greatly improved dexterity gained by maturing children. According to Baker et al., the increase in oscillatory coherence in the 20Hz band may prove to be particularly effective in enabling cortico-spinal neurons to recruit a greater number of target motor neurons (Baker et al. 1999).

Motor control appears then to involve important maturational processes throughout the lifetime of the individual and particularly during adolescent ages. Although we now have a good idea of what happens at the synaptic, behavioural, and synergistic level of neurons during these years, strong causal evidence as to the precise impact of synaptogenesis during puberty on oscillations and motor command has not yet been accurately quantified. The difficulty of isolating synaptic change, cell death and migration in vivo, and in conjunction, record their impact on brain function and behaviour constitutes a significant challenge for neuro-physiological studies. Since Turing's insightful work on investigative methods for the formal modelling of cellular development via chemical dynamics, there has been a gaining interest in complementing our formal descriptions of epigenetic mechanisms and manners in which to test them (Turing 1952). The computer, has obviously become a prime candidate for the latter. With respect to oscillatory dynamics from neural aggregates, Wilson & Cowan, are undoubtedly pioneers. Although no actual computer modelling was used per say; the formalization of the dynamics was rigourously analysed (Wilson & Cowan 1972). Indeed accurate mathematical analysis of formal models is essential practice so to identify the behavioural or informational characteristics of a system. If the complexity of a model's dynamics renders this impossible, then accurate computer simulation constitutes an ideal method for the grasping of this. In effect, one needs only the model's definition and initial conditions so to obtain a 'picture' of the projected behaviour. For this reason, by deriving a comprehensive model from our current neural and physiological knowledge

of human cognitive and motor activity, it should become possible via simulation to acquire a deeper understanding of the phenomena involved in motor action. A notable achievement in this regard was accomplished in 2007 by Richard Potter, where a multi stage model of cortical control for muscle contraction was proposed (Potter 2007). His simulation comprised of a population of simple integrate and fire cortical neurons, connected to a pool of 100 α motor neurons of the spinal tract, which generated an input of realistic inter-spike intervals for a muscle model that in turn would produce potentially applicable forces for limb contraction. The integrative nature of this work at multiple levels of neural and muscle dynamics proves that multi stage modelling can potentially provide new insights as to the mechanisms underlying behaviour and cognition or otherwise highlight the knowledge that we still lack. In line with this motivation, I propose in the following a model of neural connectivity for layer II and III of the primary motor cortex. Instead of looking at spatial integration of mechanisms over the entire nervous system for motor control, I intend to investigate the integration over time of realistic cortical neurons during development, and in particular the impact of synaptic change on oscillatory activity.

Chapter 2

Modelling Oscillatory Activity in the Primary Motor Cortex

Although the literature on artificial neural network modelling is vast it has primarily been concerned in the past with rate coding schemes. As mentioned above, this method expects biological neurons to encode information conveyed by a neuron or group of neurons as its average firing rate. Although this certainly is correlated to real neuron functioning, I support here the claim that it is by no means the only form of functional encoding undertaken by biological neural networks. Instead, I believe it is necessary to investigate not only realistic models of neural signalling, but also how they act as a cooperative whole. Not only should this make it possible to model realistic rate coding schemes but spatio-temporal ones as well. Here, I first introduce the neuron model, followed by the network model. I then present the experimental setup of various simulations, and finally discuss the obtained results.

2.1 Model

Pauluis et al. elaborated a conductance based integrate and fire model of cortical neurons founded on cytological properties of layer II and layer III of the neocortex (Pauluis et al. 1999). By simulating a sheet of 10,000 neurons, their aim was to demonstrate that synchronized firing activity could emerge from the mass action of cortical neurons alone. With successful results, this further supports the claim that thalamo-cortical oscillatory drive is not necessary for cortical oscillations nor for their coherent firing. Amongst the most important confirmation from their findings, stems from the observation that inhibitory neural firing is crucial for the emergence of rhythmic activity. This is supported by the notion that provided sufficiently strong inhibitory signals, inhibitory post synaptic potentiations (IPSPs) can sustain controlled firing and prevent signal dissipation or over excitation. In particular Pauluis et al. made use of a population constituted by 15% strong inhibitive neurons versus 85% excitatory.

2.1.1 Neuron Model

The neuron model is designed according to Pauluis et al.'s specifications. As seen in the section on cortical motor neurons, a cell's potential is described as the relation between conductance of the ion gates, current voltage and rest voltage. Each neuron has a base conductive and resting

behaviour,

$$I_r = g_r(V_m - E_r) \tag{2.1}$$

where I_r specifies the resting current, g_r the resting (leak) conductance state of the ion gates, E_r the resting potential, and V_m the current membrane potential. Because neurons can receive both inhibitive or excitative input, it is important to add a relation which dictates how the current will be affected with respect to the change in conductance. This is accomplished by summing individual terms from excitation and inhibition to the resting value. Hence we obtain,

$$I = g_r(V_m - E_r) + g_e(V_m - E_e) + g_i(V_m - E_i) \tag{2.2}$$

where I is the summed current of the neuron, g_e the excitatory conductance, E_e the excitatory resting potential, g_i the inhibitory conductance, E_i the inhibitory resting potential. As discussed in the previous chapter, the cell's signal will be excitatory if $E_e > V_m$, hence we set $E_e = 0mV$ (millivolt). Likewise, the signal will be inhibitory if $E_i < V_m$, hence we set $E_i = -80mV$. By keeping the resting conductance g_r to some positive value, and the equilibrium potential $E_r = -70mV$, the cell membrane will systematically return to the resting potential of $-90mV$ after stimulation. This stimulation then can be excitatory by setting g_e to a positive value or inhibitory by setting g_i to a positive value. Because the current flowing through the membrane changes over time a capacitive effect dampens the change in potential of the membrane with respect to the current and time. This capacitive value is determined by the membrane resistance R_m and the membrane time constant tau, where $C = R_m * tau$. A dendritic input is also added to the somatic current via I_{ds} (see below). The change in membrane potential over time is thus formulated as a differential equation of the form,

$$C\frac{\partial V}{\partial t} = g_r(V_m - E_r) + g_e(V_m - E_e) + g_i(V_m - E_i) + I_{ds} \tag{2.3}$$

This relation however doesn't take into account the fact that excitatory conductance g_e and inhibitory conductance g_i also change over time, with respect to synaptic neurotransmitter ion gate binding. This change can be expressed as a simple linear differential equation of the form,

$$\frac{\partial g_e}{\partial t} = \frac{-g_e}{tauge} \tag{2.4}$$

$$\frac{\partial g_i}{\partial t} = \frac{-g_i}{taugi} \tag{2.5}$$

where $tauge = 0.25ms$ is the conductance time constant for excitatory ion gates which cause depolarization of the membrane, and $taugi = 0.75ms$ the conductance time constant for inhibitory ion gates causing hyperpolarization of the membrane. The dynamics of this set of equations accurately describe the effects of synaptic activation at the soma of a nerve cell. Pyramidal cells of the cortex though, posses a large dendritic tree receiving connections from a large number of axons. To simulate this a two compartment model can be used: the first compartment for somatic connections and the second compartment for dendritic connections (Pauluis et al. 1999). To do this equation 2.3 can be computed with different capacitative parameters. In particular I use $R_{mse} = 600M\Omega$ $(\pm 5\% CV)$ for the somatic membrane resistance of excitatory input,

and $R_{mde} = 2.4 * R_{mse}$ for the dendritic membrane resistance of excitatory input. Similarly $R_{msi} = 800M\Omega$ ($\pm 5\% CV$) for inhibition on the soma, and $R_{mdi} = 2.4 * R_{msi}$ for the inhibition on the dendritic compartment similar to Pauluis et al. Resting conductance of somatic ion gates is $g_{ls} = 10nS$, and for dendritic conductance rest is $g_{ld} = 5nS$. For the somatic membrane time constant of excitatory post synaptic potentials (EPSPs) we set $tau_{se} = 10ms$, and $tau_{si} = 7.5ms$ for IPSPs. For dendritic compartments we set $tau_{de} = 2ms$ for EPSPs, and $tau_{di} = 1.5ms$ for IPSPs.

The current that flows from the dendritic side to the soma can also be expressed as a differential equation,

$$tau_I \frac{\partial I_{ds}}{\partial t} = -I_{ds} + (\frac{V_d - V_s}{R_{md}}) \tag{2.6}$$

where I_{ds} is the current flowing form the dendrites to the soma, V_d the dendritic membrane potential, V_s the somatic membrane potential, R_{md} the dendritic membrane resistance (R_{mdi} or R_{mde}), and $tau_I = 0.1ms$ (millisecond) the current flow time constant. The initial current value for I_{ds} is initialized at 0.0mA. Finally, neuron potentials are initialized to $-70mV(\pm 3mVSD)$, with resting potential $-70mV$, firing threshold at $-55mV$, reset value of $-90mV$, and a refractory period of $1ms$.

Now that an accurate formalization of single neurons is described, it is possible to inspect the required parameters and initial conditions for a realistic population of cortical neurons.

2.1.2 Network Model

In the present approach a two dimensional neural sheet of 10,000 neurons is implemented and meant to mimic a cortical surface of area $500\mu m * 500\mu m$ from layer II and III of the motor cortex. 85% generated EPSPs on their target whereas 15% generated IPSPs on target neurons. This reflects the proportion of excitatory versus inhibitory cell found in the motor cortex (Abeles 1991, p.50-53). Ideally, to model realistic dynamics in neurons of the motor cortex, a population of stellate, pyramidal, and fusiform cells should be arranged in three dimensions over the six cortical layers. Because I do no aim to simulate the entire activity of the primary motor cortex but simply investigate local dynamics of it, a sheet of 10,000 neurons is sufficient. Neurons are interconnected randomly with probabilities that differ depending on the originating neuron type (excitatory or inhibitory), the target type, and the target compartment, see table 2.1,

P($Excit \rightarrow Inhib_{soma}$)	0.13
P($Excit \rightarrow Inhib_{dendrite}$)	0.87
P($Excit \rightarrow Excit_{soma}$)	0
P($Excit \rightarrow Excit_{dendrite}$)	1.0
P($Inhib \rightarrow Excit_{soma}$)	0.76
P($Inhib \rightarrow Excit_{dendrite}$)	0.24
P($Inhib \rightarrow Inhib_{soma}$)	0.77
P($Inhib \rightarrow Inhib_{dendrite}$)	0.23

Table 2.1: Probability table of synaptic connections.

In their model, Pauluis et al. report that excitatory cells connect to 5% of the total target

population and inhibitory cells to 12.5%. These targets however were located within $300\mu m$ of the total space. To account for this boundary condition accurately one should compute the connection probability from table 2.1 within this radius. Because the present model was simulated using BRIAN, some limitation in this respect were met (see BRIAN in references). Sharp boundary cutoffs with respect to target connections cannot be explicitly made in BRIAN. In order to approximate this, connection weights from source to target are decreased exponentially with respect to distance; the probability of connection is then amplified to mimic a densely connected local field. Final probabilities are computed the following way,

$$P(Source \rightarrow Target) = P(table\ 2.1) * target\% * \frac{5}{3} \tag{2.7}$$

where target% corresponds to 5% for excitatory sources, or 12.5% for inhibitory sources, and 5/3 the proportional amplification ratio. Conduction delays in BRIAN are also limited[1]. Pauluis et al. originally implemented conduction velocities from a normal distribution with mean speed $0.18m.s^{-1}$ for excitatory cells, and $0.06m.s^{-1}$ for inhibitory cells. Here fixed delays had to be used on each connection. These were set to $2ms$ for excitatory sources, and $6ms$ for inhibitory source cells. Connection weights from excitatory synapses are $0.5nS$ and $1.0nS$ for inhibitory synapses.

An excitatory input of $1.0nS$ was applied to the dendritic compartment of all cells situated in the centre of the sheet over one third of the surface. This input was Poisson distributed with an input rate of 8,500 EPSPs/second. This high rate is meant to mimic non oscillatory input spike trains from other cortical regions.

2.2 Simulation

A set of 5 simulations were run; each for 2 seconds. The network was simulated using the BRIAN python library for network simulation (see BRIAN in references). The integration time step was set to 0.1ms. The spike histograms are computed after removing 200ms of initial activity to remove any potential artifacts from the initial conditions and sudden Poisson input. This is accomplished by a non-overlapping sliding window of 0.5ms. The global autocorrelation is computed thus converting time domain data into the frequency domain using a fast fourier transform (Pauluis et al. 1999). The pooled power spectrum density (PSD) is obtained by averaging the activity of the five separate runs. Numerous variations in the network configuration were tested and the set of parameters stated above gave rise to the best tested results. Correlation, phase and cumulant densities of local field potentials are analysed with NeuroSpec2.0 (Rosenberg et al. 1989, Halliday et al. 1995). Finally, all runs where performed on an Apple Mac Mini with an Intel Core Two Duo processor at 2GHz, and 2.5GB of RAM. The average run for 10,000 neurons took about 25 minutes.

2.3 Results

After a 2 second run a total of average of 48616 spikes were generated, amongst which 27352 where excitatory, and 21364 inhibitory. Hence 44% where inhibitory spikes, which is comparable

[1]BRIAN version 1.0rc4.

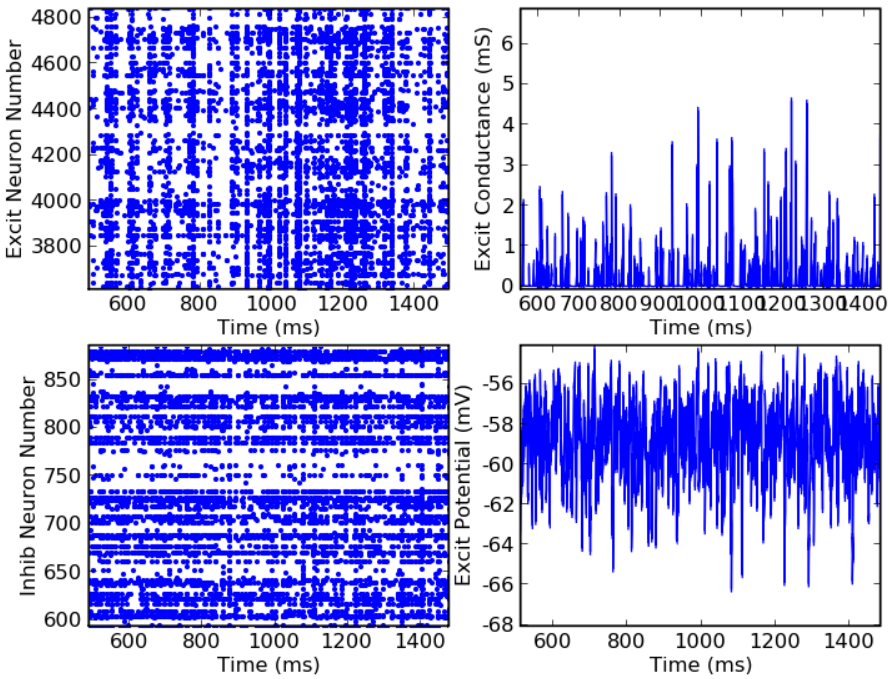

Figure 2.1: Sample spike plot for all excitatory neurons (top left), spike plot of all inhibitory neurons (bottom left), excitatory conductance changes (top right) and excitatory voltage changes for a single neuron

to the 41% obtained by Pauluis et al. Although spatial information is not seen, the plotted spike train of figure 2.1 is a good indicators of the overall firing dynamics of the network over time.

Pooled oscillatory activity in the 35-65Hz range was recorded from the overall population (figure 2.2). This is similar to the global oscillation of 65Hz obtained by Pauluis, Baker and Olivier (Pauluis et al. 1999). Differences are mostly explained by the significant sensitivity of the oscillatory frequency to propagation delays, input frequency and surface, which had to be implemented slightly differently here due to the simulation engine. In their work, Pauluis et al. varied the intensity of the Poisson input noticing that although overall rhythmic frequency does not change with respect to intensity, the number of recruited spikes is greater at higher intensity thus corresponding to a higher amplitude in the histogram and greater overall power of the spectra. This was also obtained here when the input was increased from 8,500 EPSPs/s per cell to 10,000 EPSPs/s per cell (see figure 2.2). Interestingly, not only did the power increase but the frequency band narrowed to the 45-55Hz range at 10,000 EPSPs/s. This could be due to a greater recruitment of inhibitory cells which in turn prevent excitatory cells to fire out of phase.

Pauluis et al. also applied a Poisson on the centre of the space but with Gaussian distribution. By doing so they noticed that a wider distribution required a lower input intensity than narrow distributions. Although a hard spatial limit was applied here instead of a Gaussian, by reducing this input space similar results were obtained: the oscillation band was significantly wider (7-65Hz) yet with lower average power ($\approx \frac{1}{2}$) (see figure 2.3). In their experiments, Pauluis et al. also note that conductance delays play a fundamental role on the oscillatory frequency. This is

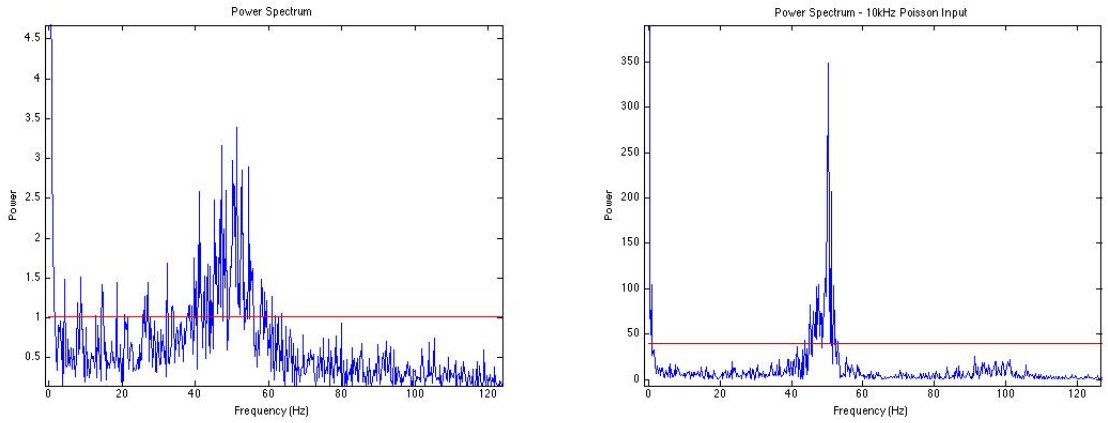

Figure 2.2: Pooled power spectral density of 10,000 neurons. Left: pool over five runs with a 8.5kHz Poisson input. Right: pool over two runs with a 10kHz Poisson input. The hard line represents $3 * SD$.

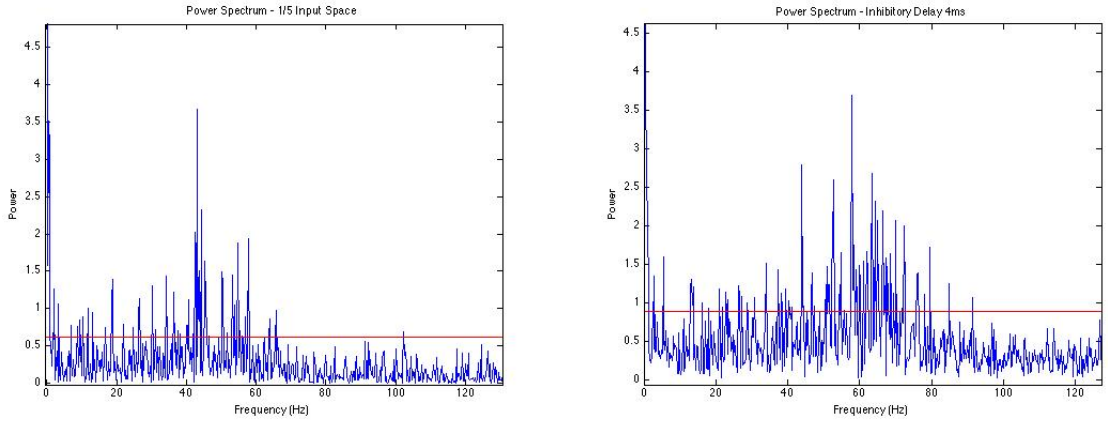

Figure 2.3: Left: spectral density with 1/5 of the spatial input. Right: spectral density with inhibitory delay reduced to 4ms pooled from two runs. The hard line represents $3 * SD$.

particularly true for inhibitory delays. By reducing the inhibitory delays they obtained higher rhythmic frequencies. To test this I ran the network with inhibitory delays reduced to 4ms while maintaining excitatory delays to 2ms. From the right plot in figure 2.3, we notice that the oscillatory band increases to a higher frequency range of 45-80Hz. This agrees with the results from Pauluis, Baker and Olivier since the global rhythm increased with shorter delays for inhibitory signals. Interestingly we notice that the amount of excitatory cells firing is reduced under two conditions. If the input intensity is too low, then a much greater number of inhibitory cells fire, but at a specific threshold this disappears. Similarly by reducing the delay of the inhibitory connections too low, such as 2ms, a sudden drop in excitatory activity is noticed. In both cases this seems to be due to an 'overpowering' of the inhibitory neurons on the excitatory population at a specific threshold. This behaviour was also noted by Pauluis et al.

Although general oscillatory activity is obtained in this model, the analysis above cannot account for the existence of strong synchronous activity, this is because the fast fourier transform of the histogram may potentially convolute different frequencies of separate cell groups into a global component. In order to examine whether an emergent synergistic event is present in the range 35-65Hz, it is necessary to examine the coherence between small spatial groups of the

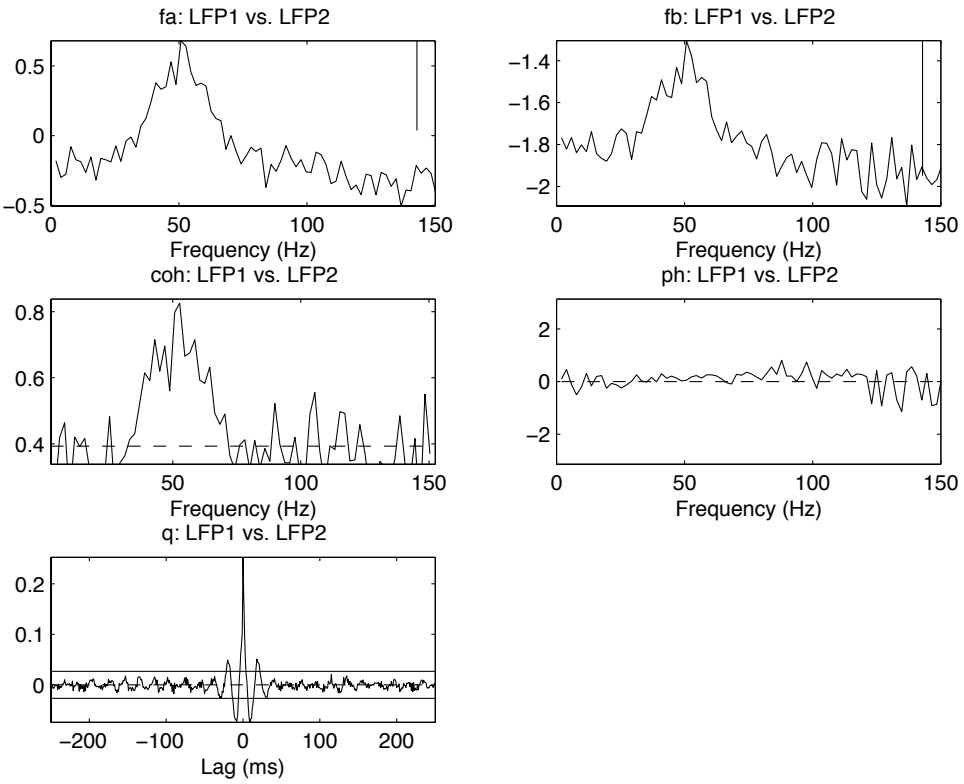

Figure 2.4: Local Field Potential comparison of inhibitory neurons with 100 neurons per field pooled from 5 runs. Top left: spectra of local field 1. Top right: spectra of local field 2. Middle left: coherence estimate between both local field. Middle right: phase difference. Bottom left: cumulant density.

network. To do so, two randomly selected local field potentials are compared in terms of spectral density, coherence, phase and cumulant density. Figure 2.4 illustrates the results obtained from two non-overlapping selected fields in the inhibitory population from a pool of 5 runs [2]. Although fields are selected randomly, only those which displayed firing activity where selected for analysis. We first notice that the spectra of each field is clearly centred on the same wave band as the total population, i.e. 35-65Hz, with a particularly strong component at approximately 54Hz. The correlation diagram indicates a strongest correlation between both local fields at the same frequency. This is confirmed by the phase diagram which displays phase locking also at around 50Hz. These results then seem to confirm that coherent oscillatory activity can emerge in cortical neural networks with spiking activity as originally postulated by Wilson and Cowan (Wilson & Cowan 1972). Indeed inhibitory connections appear to play a crucial role for this coherent oscillatory activity to take place without external rhythmic input.

Additionally, it would be interesting to investigate ways in which neural synergies, even in such small populations, may serve to control skeletal muscles and potentially be used to simulate hand grasping, or isometric finger contraction as explored by Farmer et al. (2007). A rhythmic drive from betz cells in the lower layers of the primary motor cortex, may possibly be driven by competing synergetic groups at higher levels of the cortex. Because betz cells are much larger

[2]The location of field one is (31, 6) and field two is (38, 19) from the inhibitory space of dimension (50, 30). Similar results were obtained from other local field regions such as (14, 13) and (35, 22).

these could trigger sufficiently large action potentials to drive cortico-spinal motor neuron pools. From these signals, muscle fibres sensitive to α motor neurons inter-spike-intervals may contract a limb (Potter 2007). It should be important however, to gain a better understanding of dynamic transients in oscillatory activity as this may prove fundamental for the sequential organization of voluntary motor tasks.

Now that a plausible model of coherent oscillatory activity for the motor cortex has been proposed and proven, it would be of interest to explore the extent to which it may serve as a platform to study the developmental aspect of motor control in the cortex.

Chapter 3

Modelling Developmental Impacts

As mentioned in the section on maturation of the nervous system, the brain undergoes significant changes during puberty. Gotgay et al. obtained detailed imagery of the brain's neocortex, showing how cortical thickness diminishes during puberty (Gotgay et al. 2004). Although no detailed description is given as to which cortical layers are affected and how this change affects them cytologically, a significant linear decrease in gray matter was noted in the primary motor cortex overall. As discussed above this decrease can be estimated to roughly 34% form the age of 5 to 20. Importantly they attribute this change to a decrepitude of synaptic connections between cortical neurons. Unfortunately, a number of questions are still left unclear. It may be possible that simply the least functionally significant dendritic trees spanning from nerve cells are eliminated over time. Alternatively it is possible that sexual steroids actively regulate the death of nerve cells that are least used as is has been observe in the rat's primary visual cortex (Nunez et al. 2002). Even less clear, is whether a different effect of age is exercised on different cells and their type of neurotransmitters. It may be possible for instance that cholinergic transmission is reduced or a contrario that GABAergic transmission is the one affected. The fact is that little is known as to the mechanisms responsible for puberty onset prior to the release of ganadotropin releasing hormones (GnRH) by the hypothalamic neurons (Sisk & Foster 2004). Taking this into consideration, it would be interesting to explore a variety of mechanisms by which gray matter reduction could take place in the model considered herein.

In order to validate this potential mechanism it would be appropriate to control the results obtained with biologically realistic data concerning oscillatory activity in the primary motor cortex. Findings by Gasser et al. suggest that the spectral power of high alpha and beta waves in the primary motor cortex increase over adolescence (Gasser et al. 1988). This is corroborated by experimental results from Farmer et al. which show that coherence in the 20Hz oscillatory range is accentuated between ages of 7 and 14. This suggests that early puberty in the primary motor cortex has the strongest impact on mid to high frequency oscillations. To explore the possible effect of age on synchronized neural firing I test in the following three alternate mechanisms potentially responsible the reduction in cortical gray matter.

3.1 Model

With the neuron and network model proposed in the previous chapter, there are a number of different ways one can experiment on neuropil reduction. The first method I aim to investigate

here is to compare the effects by simply reducing the total number of neurons in the neural sheet, thus simulating population wide neural death. To do so the neuron model and network architecture with 10,000 cells described in the previous chapter is used as reference and compared to the activity of a network with a 34% reduction of cells, i.e. 6600 cells. If the proportion of excitatory and inhibitory cells is maintained to 85% and 15% respectively, then 5610 excitatory cells populate the sheet versus 990 inhibitory.

The second approach consists of reducing the population of excitatory cells only. A 34% of total neural loss cannot be due to inhibitory neuron death alone since it would deplete the entire inhibitory neuron population, hence if this biased cell death process occurs in vivo, it can involve excitatory cells alone. Therefor 3400 neurons of the excitatory population are removed, leading to total population of 6600 cells with 5100 excitatory and 1500 inhibitory.

The third approach is to focus the depletion of neuropil on the network connections. Reducing the connection density should simulate a more gentle reduction in gray matter. Because I aim here to reduce gray matter density without removing cell bodies, a greater amount of synaptic 'matter' should be removed. This can be accomplished by reducing the synaptic connection probability by about 40%. Interestingly this can be done for both excitatory and inhibitory connections, or distinctively for excitatory cells or alternatively inhibitory cells alone. Results from this simulation may indicate then that the mechanism potentially responsible for synaptic elimination such as sexual hormones, internal cell regulation clock, or simply electrical activation is or isn't biased towards cholinergic or GABAergic transmission.

As in the previous simulation, a Poisson input with intensity 8,500 EPSPs/second per cell is applied to one third of the population in the centre of the sheet. Connection probabilities are also maintained except in the synaptic connectivity reduction case (see below).

3.2 Simulation

Identical to the simulation method describe in chapter 2, runs computed 2 seconds of network activity. Data in each scenario is collected from pools of 5 runs. The autocorrelation is computed using fast fourier transforms from spike time histograms in order to obtain the power spectra from pooled runs. Local field potential correlation is also computed from the pool using NeuroSpec2.0. Local fields are randomly selected and have cover a surface of 100 neurons. Importance of coherence difference is calculated by taking the difference in coherence between two activity pools and verifying significance by comparing the activity to $3*$ standard deviation.

3.3 Results

3.3.1 Results from Proportional Cell Reduction

In the first experiment, the number of excitatory and inhibitory cells where reduced by 34%, to a total of 6600 nerve cells. There are then 5610 excitatory cells (85%) and 990 inhibitory cells (15%). Local field potentials are then computed for two randomly selected non-overlapping local fields of the inhibitory population[1]. Figure 3.1 shows that significant power spectra is maintained in the 35-65Hz frequency band in the proportionally reduced population of cells. Also coherence

[1]Local field 1 at (22,6) and local field 2 at (11,7)

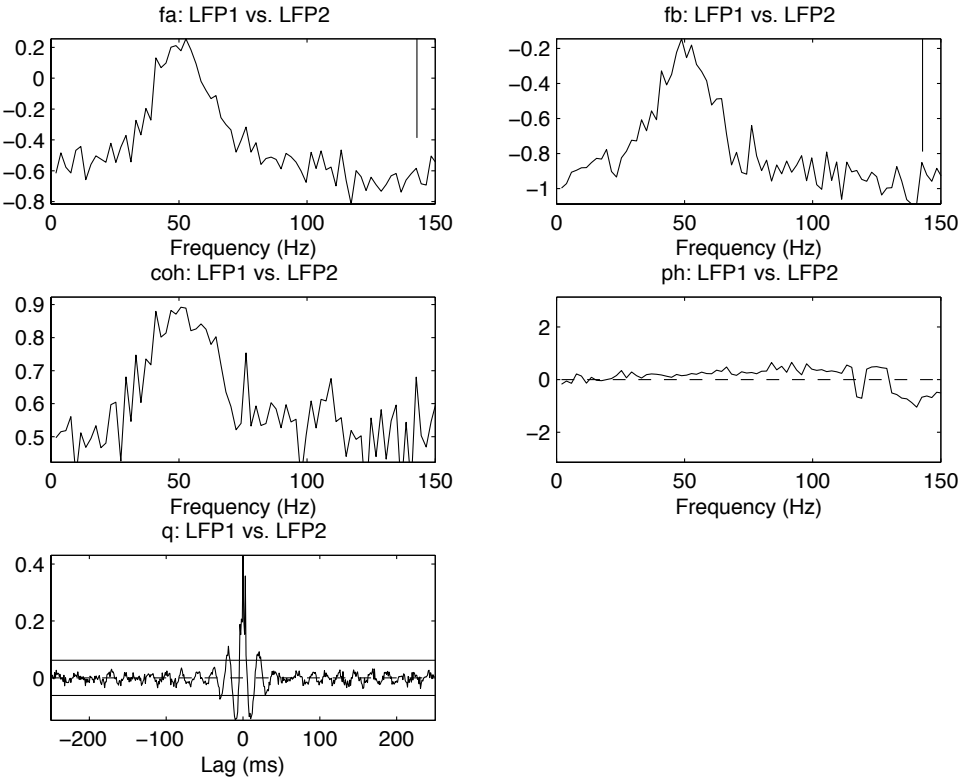

Figure 3.1: Local Field comparison data of a network of 6600 neurons, with proportionally reduced excitatory and inhibitory neurons with local field 1 at (22,6) and local field 2 at (11,7).

in the nerve cell activity is clearly taking place the same frequency band as is shown by the middle left plot.

This in turn can be compared to the activity of the same local fields in the 10,000 neuron population network shown in figure 3.2, which also shows strong oscillations and coherence in the 35-65Hz frequency band. Because the spatial dimensions of the inhibitory neurons has size (33, 30), it is necessary to scale the *x-axis* to the appropriate location of the spatial layout of the larger sheet of (50, 30) inhibitory neurons. This explains why on the larger sheet, the local fields have *x-coordinate* $33 = 22 * \frac{50}{33}$ and $17 = 11 * \frac{50}{33}$ respectively. The *y-axis* between sheets are of equal dimension and therefor remain unchanged.

Because the present work aims at observing any potential developmental change with respect to synergetic behaviour, it is most useful to carefully consider the comparative coherent behaviour between the network of 10,000 neurons and the network containing only 6,600. It is difficult however, to assess this purely on by observing the coherence output of individual local field comparisons. For this reason it may be useful to compute the exact difference between the coherence vector of the smaller network with that of the larger one. Figure 3.3 illustrates the comparative coherence between both networks by computing,

$$\delta = coh(N_{6,600}) - coh(N_{10,000}) \tag{3.1}$$

where $coh(N)$ provides the coherence of two local field potentials of network N, $N_{6,600}$ denotes

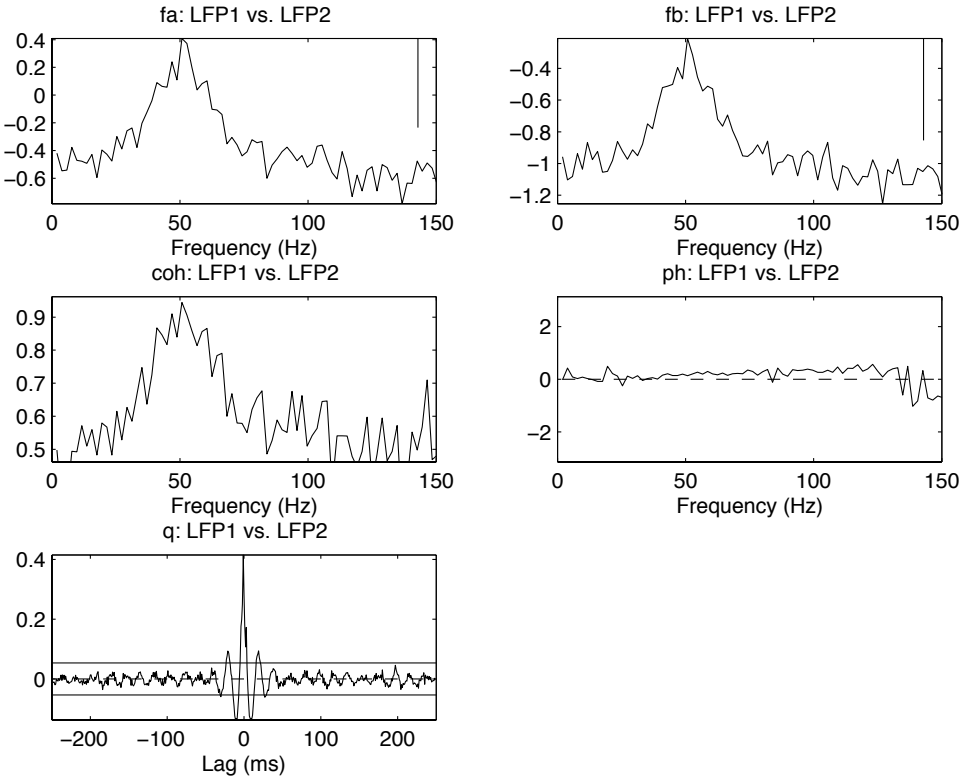

Figure 3.2: Local Field comparison data of a network of 10,000 neurons with local field 1 at (33,6) and local field 2 at (17,7).

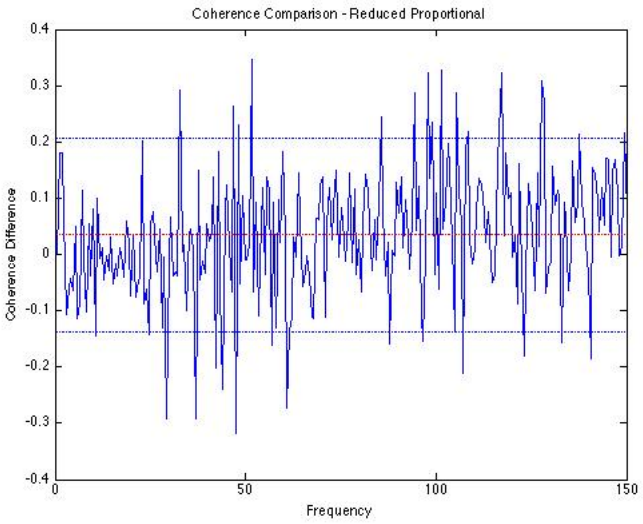

Figure 3.3: Local field coherence comparison between the network of population 6,600 with the network of population 10,000. Horizontal red line is the mean; horizontal blue lines are $3 * SD$ from the mean.

the network of 6,600 cells, and $N_{10,000}$ the network of 10,000 cells. Hence, figure 3.3 indicates the difference in coherence estimate between networks $N_{6,600}$ and $N_{10,000}$, where positive values indicate stronger coherence of local field potentials in $N_{6,600}$ than the same local fields in $N_{10,000}$. From this figure we notice then that the mean coherence is overall positive indicating that coherence has slightly increased in the population of 6,600 neurons. At first glance this may seem to support the validity and the model and appear to fit Gasser's and his colleague's biological observations. Arguably it appear that a slight coherence increase by about 35Hz and higher may be present. Because this is not restricted to the 35-65Hz band, this may seem superficial. But it seems plausible that frequencies beyond 70Hz are in fact harmonics of from the principle frequency band. This would then predict an increase in coherence in the range 70-130Hz. However because no noticeable specific increase in the 35-65Hz frequency band is present, it is difficult to claim that any significant gain in coherence has occurred. It is possible then that proportional reduction of both inhibitory and excitatory neurons is inaccurate or as least insufficient to account for stronger coherence. Alternatively, the proposed cortical neural model may be biologically inadequate, or perhaps even that a mechanism other than gray matter depletion is responsible for increased rhythmic coherence. To verify these possibilities other potential maturation schemes are explored.

3.3.2 Results from Excitatory Cell Reduction

Alternatively, the reduction in cortical gray matter of the cortex during development could be caused by an auto-regulated apoptosis of excitatory neurons. This hypothesis is not founded but the lack of biological data on the matter requires that this possibility be considered. To simulate this phenomena, the total population of network is diminished purely by removing excitatory cells from the space. The total number of cells removed corresponds to 34% of the total population, which corresponds to 3400 cells. The new cell population is therefor composed of 5100 excitatory cells ($\approx 77.3\%$) versus 1500 inhibitory cells ($\approx 22.7\%$).

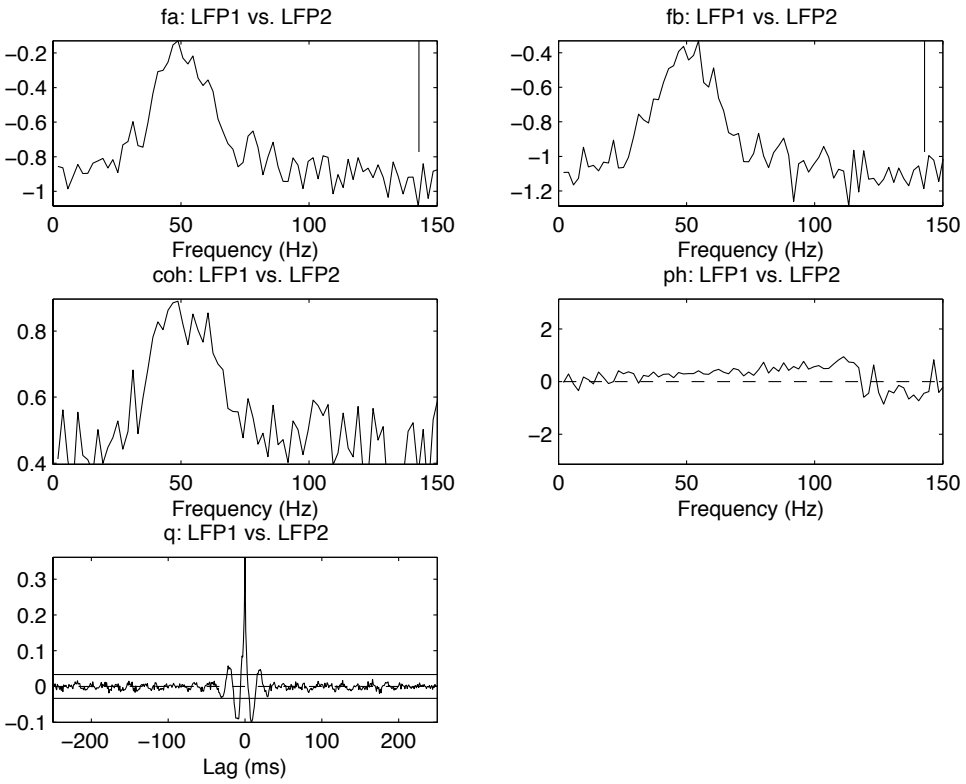

Figure 3.4: Local Field comparison data of a network of 6600 neurons, with a reduced excitatory population of 5,100 neurons and normal inhibitory population of 1500 neurons. Local field 1 at (18,11) and local field 2 at (36,8).

Similar to the previous experiments, two non-overlapping local fields are selected randomly for coherence analysis from the two networks[2]. Spectra, coherence, phase and cumulant density for the network of 6,600 cells is shown in figure 3.4. This figure shows that oscillatory activity in the range 35-65Hz is also present. The phase between both field rhythms are also closest within this range. Significant coherence also takes place in this network in the 35-65Hz range with a peak at approximately 50Hz.

For the same local field locations the high population network of 10,000 neurons also features coherent oscillations in the 35-65Hz range as expected (see figure 3.5).

To adequately assess whether this exclusive reduction of excitatory neurons has an effect on coherence, the same analytical method as in the initial experiment was employed. Coherence differences are computed following equation 3.1. This differential comparison can be seen in figure 3.6. We notice form this plot that this difference is slightly positive meaning that coherence may have become slightly stronger. But, similar to the previous results this positive difference is not accentuated in the principle frequency range of 35-65Hz. Thus no clear maturation of the oscillatory qualities of the network seems to have taken place from this kind of disproportionate reduction in the number of excitatory cells.

After completing these two experiments it seems that cell apoptosis may not be responsible for the stronger coherence observed in the mature motor cortex. Alternatively, as suggested

[2]For this experiment, local field 1 was at (18,11) and local field 2 at (36,8)

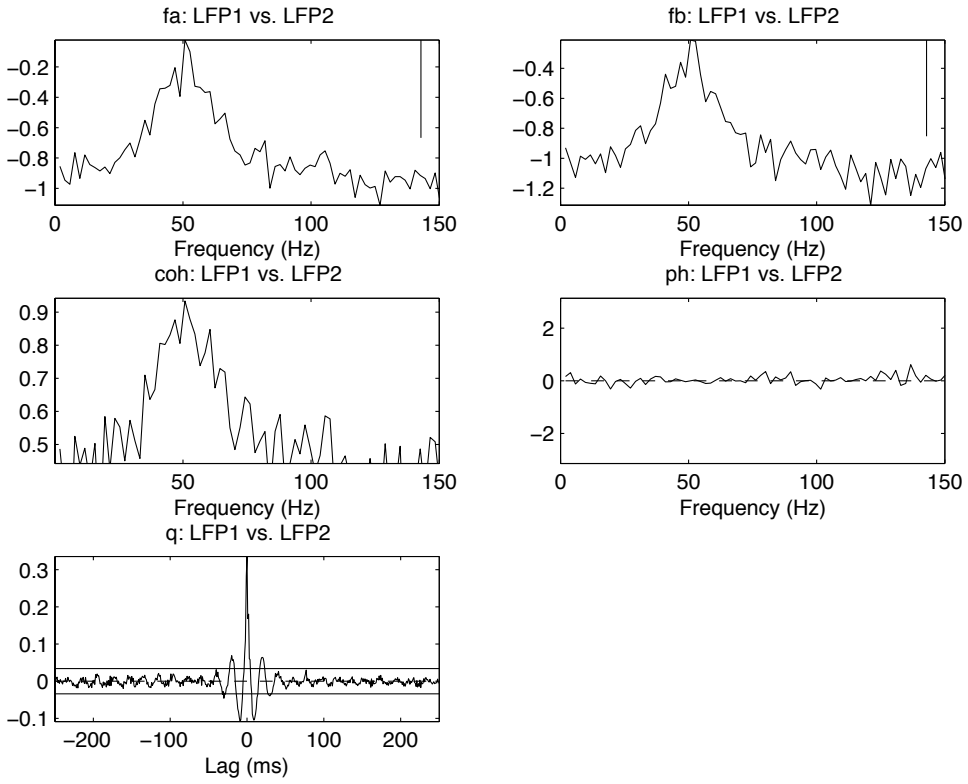

Figure 3.5: Local Field comparison data of a network of 10,000 neurons. Local field 1 at (18,11) and local field 2 at (36,8).

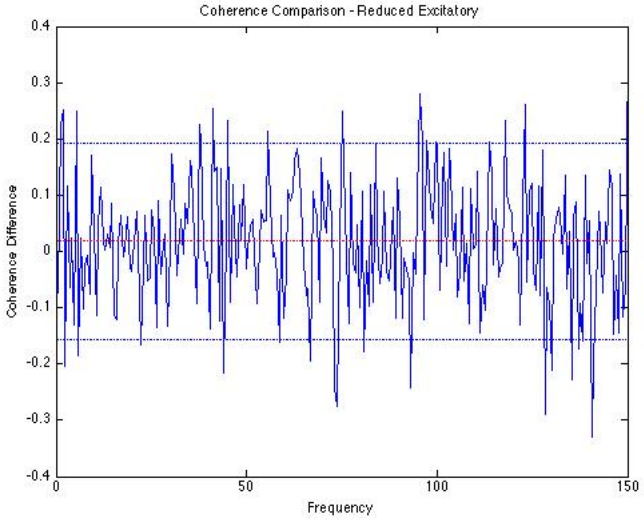

Figure 3.6: Local field coherence comparison between the disproportional network of population 6,600 with the network of population 10,000. Horizontal red line is the mean; horizontal blue lines are $3 * SD$ from the mean.

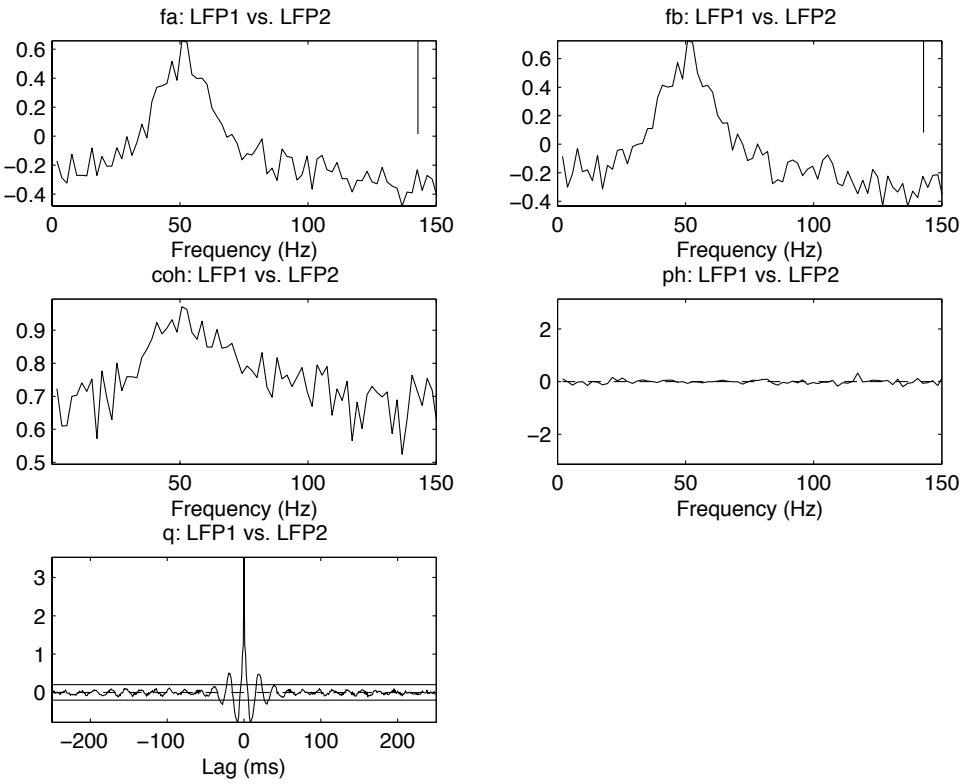

Figure 3.7: Local Field comparison data of a network of 10,000 neurons. Local field 1 at (23,23) and local field 2 at (30,9).

by Blakemore, Choudhury and others, reduction in synaptic connectivity may be a key aspect of cortical change during puberty, which would also explain the reduction of gray matter observed (Blakemore & Choudhury 2006, Gotgay et al. 2004). The following experiments aim at investigating this possibility.

3.3.3 Results from Synaptic Connectivity Reduction

In order to explore whether the change in synaptic density plays an important role in synchronized oscillations of the cortex, it is possible to modulate the connection probability that dictates the chances that any two neurons connect. Three interesting schemes should be investigated. The first involves reducing the probability that an inhibitory neuron connects to other neurons; the second is to reduce the probability that an excitatory neuron connects to other neurons; and the last is to diminish the probability that any neuron connects to any other. In the current experiments, the probability that a source neuron connects to a target was reduced by 40%. This is meant to simulate strong neuropil reduction without having to reduce the number of neuron bodies. Importantly, for the following three experiments the same local field potential locations where analysed in comparison to the standard network behaviour of 10,000 neurons describe in chapter 2; I will refer to this network as N_{std}. These locations are: (23, 23) for local field 1, and (30, 9) for local field 2. The spectral power, coherence, phase and cummulant density features of the standard network with these centre points is displayed in figure 3.7.

For the first experiment the connection probability scheme was determined using the connec-

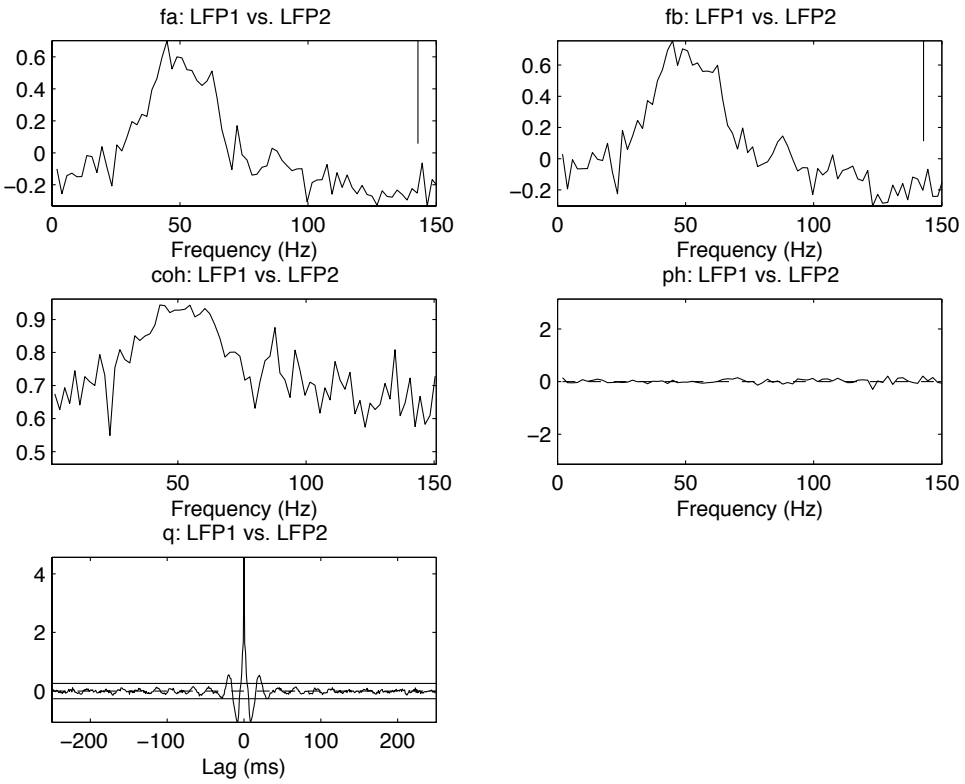

Figure 3.8: Local Field comparison data of a network of 10,000 neurons with inhibitory connections reduced by 40%. Local field 1 at (23,23) and local field 2 at (30,9).

tion probability table in chapter 2 (table 2.1), and the amplification equation 2.7. This was then adjusted for connections with inhibitory sources to the probabilities of table 3.1[3]. The number of neurons was not changed and remained at a total of 10,000 cells.

P($Inhib \rightarrow Excit_{soma}$)	0.095
P($Inhib \rightarrow Excit_{dendrite}$)	0.03
P($Inhib \rightarrow Inhib_{soma}$)	0.09625
P($Inhib \rightarrow Inhib_{dendrite}$)	0.02875

Table 3.1: Probability table for reduced inhibitory synaptic connections.

With these connectivity probabilities it is then possible to create a network with a more sparse inhibitory effects; I will refer to this network as N_{Rinh}. After running this network model over 5 pools of 2 seconds each, spectral power, phase, coherence and cumulant density were measured for two randomly selected local fields that displayed firing activity. Because both fields demonstrated significant oscillations in the range of interest (35-65Hz) but also showed that the activity was synchronized, is was reasonable to claim that this network architecture may constitute a good candidate to neural maturation (see spectral and coherence plot in figure 3.8). The differential coherence plot between N_{Rinh} and N_{std} was thus generated in order to detect any significant coherence strengthening. This analysis is shown in figure 3.9. From figure 3.9,

[3]These include the amplification adjustments of equation 2.7.

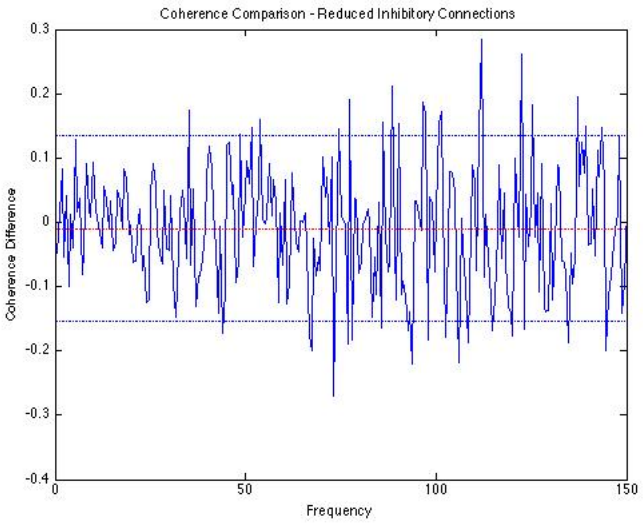

Figure 3.9: Local field coherence comparison between the reduced inhibitory connection network with the standard network of population 10,000. Horizontal red line is the mean; horizontal blue lines are $3 * SD$ from the mean.

we notice that the differential coherence is centred around the mean. In fact this coherence difference appears least different for frequencies below 75Hz. Overall however, because the mean is slightly negative (≈ -0.01) this would suggest that reducing GABAergic synapses does not accentuate neural synchrony even if this mechanism did take place during maturation.

With similar motivations, it is important to verify whether a reduction in cholinergic synapses may play a role in maturation. To do so the probability that excitatory neurons connect to a target was reduced by 40% while maintaining the normal rate of connection for inhibitory neurons. Here again the population size was maintained at 10,000 nerve cells. The connections probabilities that were changed are illustrated in table 3.2[4].

$\mathrm{P}(Excit \rightarrow Inhib_{soma})$	0.065
$\mathrm{P}(Excit \rightarrow Inhib_{dendrite})$	0.0435
$\mathrm{P}(Excit \rightarrow Excit_{soma})$	0
$\mathrm{P}(Excit \rightarrow Excit_{dendrite})$	0.05

Table 3.2: Probability table for reduced excitatory synaptic connections.

Five sample runs of 2 seconds each were recorded and analysed for this network; which I will refer to as N_{Rexc}. Two local field potentials at positions (23, 23) and (30, 9) where used to verify that synchronous oscillatory activity did occur in the range 35-65Hz (see figure 3.10). After which the differential coherence between N_{Rexc} and N_{std} was computed as shown in figure 3.11. From figure 3.11 we notice that this network displays a significantly more negative mean than network N_{Rinh} at about -0.09. This shows that a reduction in excitatory connectivity reduces coherence more significantly than reduced inhibitory connectivity. Furthermore, no other particularly significant activity seems to take place at any frequency band. These results eliminate the possibility that potential cholinergic targeting steroids or cell regulation would

[4]These include the amplification adjustments of equation 2.7.

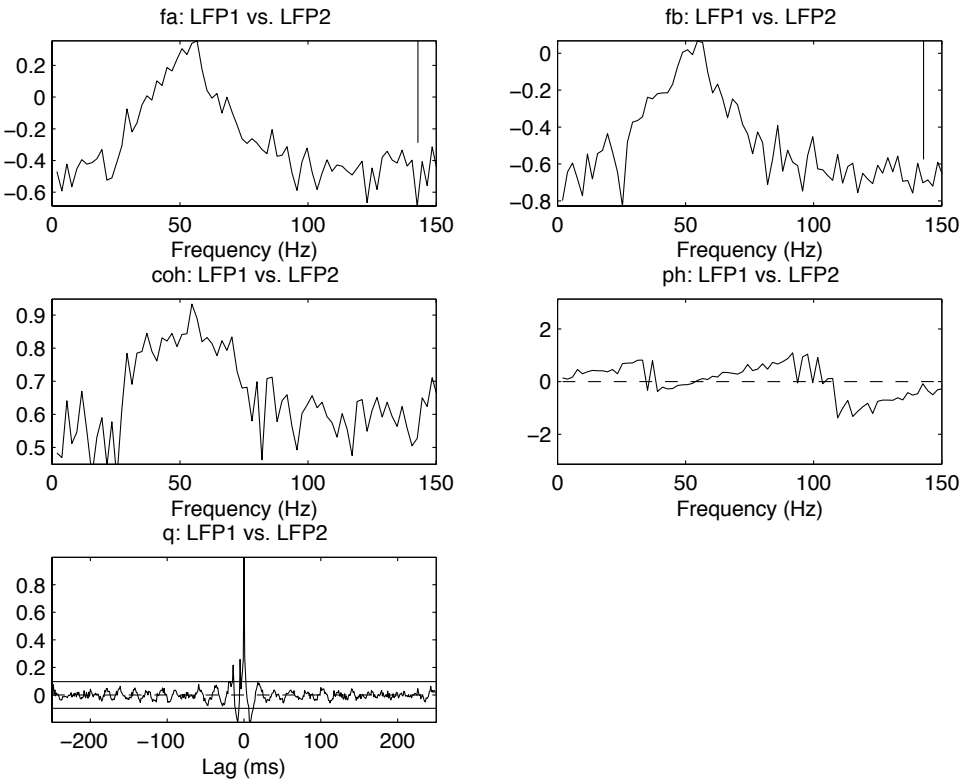

Figure 3.10: Local Field comparison data of a network of 10,000 neurons with excitatory connections reduced by 40%. Local field 1 at (23,23) and local field 2 at (30,9).

influence the appearance of stronger and better defined synchronous activity in the motor cortex during maturation.

Finally, to eliminate the possibility that strong coherent rhythms emerge due to the combined effect of reduced synaptic connectivity of both excitatory and inhibitory type, both connections types were reduced by 40% in network that I will refer to as N_{Rall}. For this network architecture both connection probabilities from table 3.1 and table 3.2 are used to define the connections topology. The spectral analysis of the same local field potentials was again obtained and displayed weak but existing power spectra in the 35-65Hz band. As illustrated by figure 3.12, coherence was just as strong however between both local fields. By analysing the differential coherence between N_{Rall} and N_{std} we notice that the coherence is even more negative than in the previous two cases. Figure 3.13 shows a mean difference at about -0.019. This further supports the claim that synaptic reduction cannot contribute to strengthening oscillatory coherence during puberty.

3.4 Discussion

Taken together we notice that the best candidate for increasing coherent activity in the motor cortex during adolescence is the scenario where cellular death afflicts both excitatory and inhibitory neurons. This was demonstrated by the first experiment. There are limitations as to the validity of this claim however. Although the results from the first experiment show a

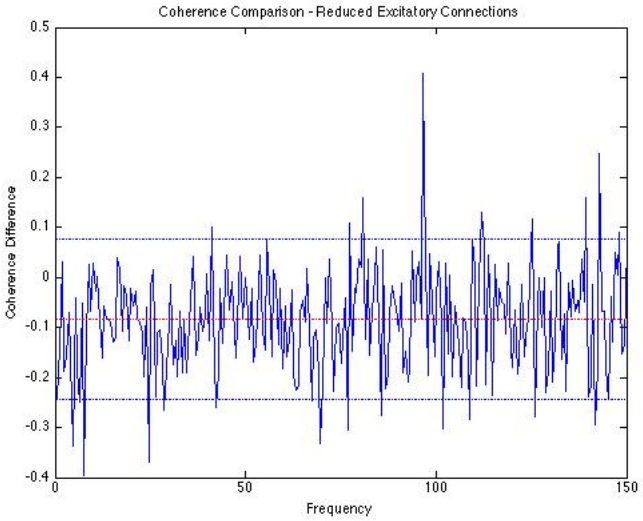

Figure 3.11: Local field coherence comparison between the reduced excitatory connection network with the standard network of population 10,000. Horizontal red line is the mean; horizontal blue lines are $3 * SD$ from the mean.

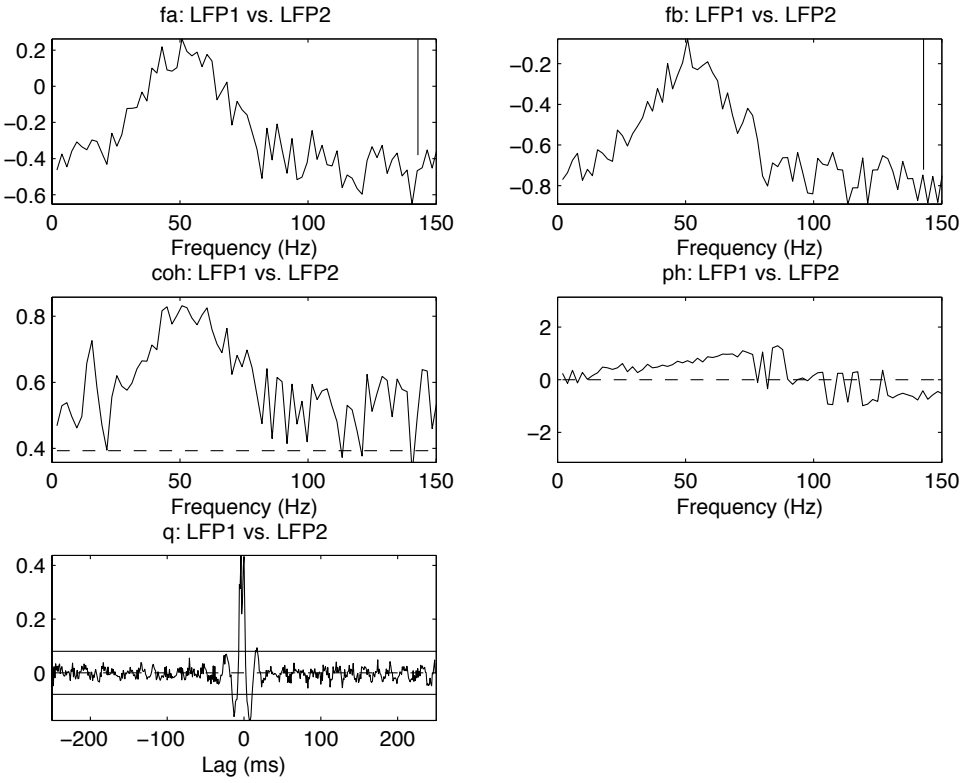

Figure 3.12: Local Field comparison data of a network of 10,000 neurons with all connections reduced by 40%. Local field 1 at (23,23) and local field 2 at (30,9).

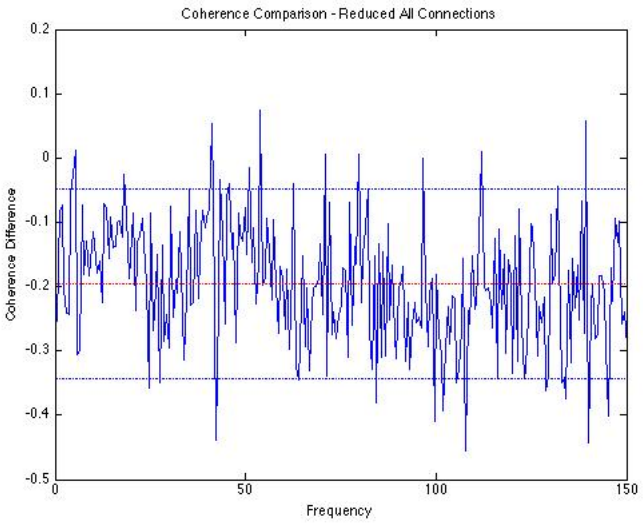

Figure 3.13: Local field coherence comparison between the globally reduced connection network with the standard network of population 10,000. Horizontal red line is the mean; horizontal blue lines are $3 * SD$ from the mean.

positive mean differential coherence, there is no significant sign of strengthening in the range of the principle frequency component (35-65Hz). Instead the noticed increase in coherence appears to affect nearly all frequencies of the network. Arguably from figure 3.3 it appears that a slight strengthening in oscillatory synchrony occurs in activity above 35Hz. This may imply that not only coherence is gained in the range 35-65Hz of the principle wave band, but also in harmonic frequencies of 70-130Hz. A more sophisticated method of analysis may help clarify this possibility.

The lack of clear gain in the coherence may otherwise be attributed to the neuron or network model employed. With respect to the neuron model, a simplification was made in the synaptic connectivity reduction experiments: what the simulation eliminated was axonal connections to the target dendritic or somatic compartment of a neuron. A single axon however main create multiple connections per neuron, and the same axon may affect more than a single neuron. To account for realistic synaptic reduction, a multi dendritic compartment model could be employed; in which case a subset of dendrites may then be removed without terminating the entire connection to the target neuron. The potential impact of this on the quality of the model for the purpose of spatio-temporal coding are not known however. Another possibility that has been largely ignored in the present model, is that specialization in of neurons appears to occur in parallel to cell and synaptic decrease during puberty (Blakemore & Choudhury 2006). Connection strengthening may play a key role in amplifying the coherent phase in the majority of local neuron pools. This could potentially be simulated by implementing a mechanism for real time synaptic plasticity. It may be possible through such a mechanism that disparate firing caused by numerous week local connections may 'channel' into a single strong connection in adolescent neural dynamics. This could potentially give rise to strong coordinated activity which would in turn amplify the coherence.

In the current network model, reduction of cell number implied a redistribution of the neurons in a uniform way in the two dimensional space. Because of this, spatial conditions are not faith-

fully preserved when simulating neural death. The conservation of spatial topology is not only more biologically realistic, but it also appears to play an important role in the neural dynamics of the proposed model. Hence the lack of accurate spatial consideration might have affected the nature of the obtained results. However, when testing for synaptic reduction the number of neurons was maintained equal: reducing the connection probability induced a more sparse network which ultimately isolates neurons previously connected. This should have constituted an accurate spatial condition, yet no maturational effect on oscillatory activity was detected in these schemes.

Overall it appears that to explore developmental aspects of cortical dynamics, it would be useful to not only devise a stronger set of analytical tools, but also explore alternate configurations of the neuron and network models.

Chapter 4

Conclusion

Science has still a lot of work to do to gain a profound understanding of the mechanisms involved in human behaviour. It seems however, that achieving such an understanding could give rise to new insights as to the fundamental principles of intelligence and adaptation. For this endeavour it is important not to omit the context in which the system under scrutiny is situated. The recent enthusiasm towards situated and embodied cognition is a positive response to this concern. This approach aims to conciliate abstract, and at times, normative interpretations of mechanisms underlying behaviour and cognition, with the concrete observable. Often however, the complex phenomena that we observe are not the outcome of complex yet temporally fixed systems, but manifestations of these systems' aptitudes as they develop over an extended time. The aim of the present study was to explore the ways in which we can model such long term dynamic transients in the brain so as to better understand it. In the first chapter I have given a broad review of anatomical features of the nervous system responsible for motor control. I then focussed the attention to formal aspects of nerve cell modelling. This allowed for the introduction of fundamental work in neural dynamics at the single cell, but also at the level of an entire population. In particular, the notion of oscillatory activity as a pervasive phenomena in the nervous system was introduced along with functional implications that such synergetic rhythms may have for sensation, behaviour and thought. Key aspects of neural development is then outlined with an emphasis on the important role that it has been shown to play on oscillatory activity in the brain and in particular on muscle control. The following chapter proposed a biologically based neural and network model of spiking neurons which, via computer simulation, gives rise to emergent coherent oscillations in a population of 10,000 cells. The possibility that development mechanisms may give rise in this model to a realistic gain in coherent activity was explored. Although some experiments have shown potentially significant results, no clear strengthening of coherent activity could be determined. Suggestions as to the reasons possibly involved in this outcome were finally discussed.

In addition, I believe it is fair to recognize that this work motivates further exploration into the realm of emergent phenomena from cognitive mechanisms. My view is that until a satisfactory account for human behaviour and thought can be achieved, even within a particular domain, we cannot rule out the possibility that yet unknown complex phenomena may further emerge from properly understood and simulated dynamics of component parts. My hope is that a better understanding in chemical dynamics, epigenetic mechanisms, population dynamics and alike, will provide crucial insight as to the fundamental principles of human adaptive behaviour.

References

Abeles, M. (1991). Corticonics: Neural circuits of the cerebral cortex. Cambridge University Press.

Ashby, W. R. (1956). An Introduction to Cybernetics, (Chapman & Hall, London). p. 207.

Baker, S. N., Kilner, J. M., Pinches, E. M., Lemon, R. N. (1999). The role of synchrony and oscillations in the motor output. Exp. Brain. Res. 128: 109-117.

Baldissera, F., Hultborn, H., Illert, M. (1981). Integration in spinal neural systems. In V. B. Brooks (Ed.), Hanbook of physiology (Sec. 1, Vol. II, p. 509-597). Baltimore: Williams & Wilkins.

Barlow, H. B. (1972). Single units and sensation: A neuron doctrine for perceptual psychology? Perception. 1: 371-394.

Bazhenov, M., Timofeev, I. (2006). Thalamocortical oscillations. Scholarpedia, 1(6): 1319.

Bedau, A. M. (1997). Weak Emergence. In James Tomberlin, ed., 1997, Philosophical Perspectives: Mind, Causation, and World, Blackwell Publishers. 11: 375-399

Blakemore, S-J., Choudhury, S. (2006). Brain development during puberty: state of the science. Developmental Science. 9(1): 11-14.

Blinkov, S. M., Glezer, I. I. (1968). Humain brain in figgures and tables: A quantitative handbook (translated by B. Haigh). Plenum Press, New York.

Bourgeois, J.P., Goldman-Rakic, P.S., Rakic, P. (1994). Synaptogenesis in the prefrontal cortex of rhesus monkeys. Cerebral Cortex.

Buser, P., Rougeul-Buser, A. (1995). Do cortical and thalamic bioelectric oscillations have a functional role? A brief survey and discussion. J. Physiology, Paris. 89: 249-254.

Bush P., Sejnowski, T. (1996). Inhibition synchronizes sparsely connected cortical neurons within and between columns in realistic network models. Journal of Computational Neuroscience. 3: 91-110.

Churchland, P. (1986). Neurophilosophy: Toward a Unified Science of the Mind-Brain. Cambridge, MA: The MIT Press.

Churchland, P., Sejnowski, J. T., (1992). The Computational Brain. Cambridge, MA: MIT Press.

Cohen, A. H., Rossignol, S., Grillner, S. (1988). Neural control of rhythmic movements in vertebrates. New York: Wiley.

Conway, B.A., Halliday, D.M., Farmer, S.F., Shahani, U., Maas, P., Weir, A.I., Rosenberg, J.R. (1995). Synchronization between motor cortex and spinal motoneuronal pool during the performance of a maintained motor task in man. J. Physiol. 489(3): 917-24.

Deecke, L., Scheid, P., Kornhuber, H. H. (1969). Distribution of readiness potential, premotion positivity, and motor potential of the human cerebral cortex preceding voluntary finger movements. Experimental Brain Research, 7: 158-168.

Eckhorn, R., Bauer, R., Jordan, W., Brosch, M., Kruse, W., Munk, M., Reiboek, H. (1988). Coherent oscillations: A mechanism for feature linking in the visual cortex?. Biol. Cybern. 60: 121-130.

Engel, A.K., König, P., Singer, W. (1991a). Direct physiological evidence for scene segmentation by temporal coding. Proc. Nati. Acad. Sci. USA 88: 9136-9140.

Engel, A.K, Kreiter, A.K., König, P., Singer, W. (1991b). Synchronization of oscillatory neuronal responses between striate and extrastriate visual cortical areas of the cat. Proc. Natl. Acad. Sci. USA 88: 6048-6052.

Evarts, E. V. (1981). Role of motor cortex in voluntary movements in primates. In V.B. Brooks (Ed.), Handbook of physiology (Sec. 1, Vol.II, p. 1083-1120). Bethesda, MD: American Physiological Society.

Farmer, F. S., Gibbs, J., Halliday, M. D., Harrison, M. L., James, M. L., Mayston, J. M., Stephens, A. J. (2007). Changes in EMG coherence between long and short thumb abductor muscles during human development. J. Physiol. 579(2): 389-402.

Freiwald, W.A., Kreiter, A.K., Singer, W. (1995). Stimulus dependent inter-columnar synchronization of single unit responses in cat area 17. Neuroreport 6: 2348-2352.

Gasser, T., Verleger, P., Bacher, P., Sroka, L. (1988). Development of the EEG of school age children and adolescents. I. Analysis of band power. Electroencephogr. Clin. Neurophysiol. 69: 91-99.

Georgopoulos, A. P., Schwartz, A. B., Kettner, R. E. (1986). Neuronal population coding of movement direction. Science, 233: 1416-1419.

Gogtay, N., Giedd, N. J., Lusk, L., Hayashi, M. K., Greenstein, D., Vaituzis, A. C., Nugent, F. T., Herman, H. D., Clasen, S. L., Toga, W. A., Rapoport, L. J., and Thompson, M. P. (2004). Dynamic mapping of human cortical development during childhood through early adulthood. Proc. Nati. Acad. Sci. USA. 101(21): 8174 - 8179.

Halliday D.M., Rosenberg J.R., Amjad A.M., Breeze P., Conway B.A., Farmer S.F. (1995). A framework for the analysis of mixed time series/point process data - Theory and application to the study of physiological tremor, single motor unit discharges and electromyograms, Progress in Biophysics and molecular Biology, 64: 237-278.

Haugeland, John. 1985. Artificial Intelligence: The Very Idea. Cambridge, MA: MIT Press.

Hodgkin, A. L., Huxley, A. F., (1952) The Components of membrane conductance in the giant axon of Loligo. J. of Physiol. 116: 473-496.

Huttenlocher, P. R., De Courten, C., Garey, L. J., Van Der Loos, H. (1983). Synaptic development in human cerebral cortex. International Journal of Neurology, (16-17): 144-154.

Ito, M. (1984). The cerebellum and neural control. New York: Raven Press.

Jahnsen, H. and Llinas, R. (1984). Electrophysiological properties of guinea-pig thalamic neurones: an in vitro study. J. Physiol. (Lond.), 349: 205-226.

Kandel, E. R., Schwartz, J. H., Jessell, T. M. (2000). Principles of Neural Science, 4th ed. McGraw-Hill, New York.

Kelso, J. A. S. (1995). Dynamic Patterns. Cambridge, MA: MIT Press. p. 8-28.

Kreiter A.K., Singer W. (1996). On the role of neural synchrony in the primate visual cortex. In: Brain theory (Aertsen A, Braitenberg V, eds), Amsterdam: Elsevier. p. 201-227.

Lewes, G. H. (1875). written at London, Problems of Life and Mind (First Series), vol. 2, Trubner.

Luciana, M., Nelson, C. A. (1998). The functional emergence of prefrontally-guided working memory systems in four- to eight-year-old children. Neuropsychologia 36: 273-93.

Marsden, C. D. (1982). The mysterious functions of the basal ganglia: The Robert Warternberg Lecture. Neurology, 32: 514-539.

Marshall, P.J., Bar-Haim, Y., Fox, N.A. (2002). Development of the EEG from 5 months to 4 years of age. Clin. Neurophysiol. 113: 1199-1208.

Maturana, H., Varela, F. J. (1980). Autopoiesis and cognition: The realization of the living. Dordrecht, Holland: D. Reidel Publishing.

McCulloch, W., Pitts W., (1943). A Logical Calculus of the Ideas Immanent in Nervous Activity, Bulletin of Mathematical Biophysics. 5: 115-133.

McMahon, T. A. (1984). Muscles, reflexes, and locomotion. Princeton, NJ: Princeton University Press.

Morison, R. S., Bassett, D. L. (1945). Electrical activity of the thalamus and basal ganglia in decorticated cats. Journal of Neurophysiology. 5: 309-314.

Murthy, N. V., Fetz, E. E., (1992). Coherent 25- to 35-Hz oscillations in the sensorimotor cortex of awake behaving monkeys. Proc. Natl. Acad. Sci. Neurobiology. 89: 5670-5674.

Nunez, J. L., Sodhi, J., Juraska, J. M. (2002). Ovarian hormones after postnatal day 20 reduce neuron number in the rat primary visual cortex. J. Neurobiol. 52: 312-321.

Pauluis, Q., Baker, N. S., Olivier, E. (1999). Emergent oscillations in a realistic network: The role of inhibition and the effect of the spatiotemporal distribution of the input. Journal of Computational Neuroscience, 6: 25-48.

Paus, T. (2005). Mapping brain maturation and cognitive development during adolescence-Trends in Cognitive Sciences 9(2).

Penfield, W., Rasmussen, T. (1950). the cerebral cortex of man: A clinical study of localization of function. New York: Mac Millien.

Perkel, D. H., Bullock, T. H., (1968). Neural coding. Neuroscience Research Program Bulletin. 63: 221-348.

Potter, R. (2007). On Simulations of Corticospinal Projections. Master's Thesis, University of Sussex.

Purves, D., Augustine, J. G., Fitzpatrick, D., Katz, C. L., LaMantia, A-S., McNamara, O. J., Williams, S. M. (2001). Neuroscience, Second Edition. Sinauer Associates, Inc.

Ramón y Cajal, S. (1909, 1911). Histologie du Système Nerveux de l'Homme et des Vertébrés (French edition reviewed and updated by the author, translated from Spanish by L. Azoulay),

Maloine, Paris, France. This book was published in English in 1995 as Histology of the Nervous System of Man and Vertebrates (translated by N. Swanson and L.W. Swanson), Oxford University Press.

Rosenbaum, A. D. (1991). Human motor control. Academic Press. p. 52-56.

Rosenberg, J.R., Amjad, A.M., Breeze, P., Brillinger, D.R., Halliday, D.M. (1989). The fourier approach to the identification of functional coupling between neuronal spike trains, Progress in Biophysics and molecular Biology, 53: 1-31.

Rumelhart, D.E., J.L. McClelland and the PDP Research Group (1986). Parallel Distributed Processing: Explorations in the Microstructure of Cognition. Cambridge, MA: MIT Press.

Sherington, C. S., (1906). Integrative action of the nervous system. New York: Scribner.

Sisk, L. C., Foster, L. D. (2004). The neural basis of puberty and adolescence. Nature Neuroscience, 7: 1040-1047.

Sowell, R. E., Thompson, M. P., Leonard, M. C., Welcome, E. S., Kan, E., W. Toga. W. A. (2004). Longitudinal Mapping of Cortical Thickness and Brain Growth in Normal Children. The Journal of Neuroscience, 24(38): 8223- 8231.

Steriade, M. Deschenes, M. (1984). The thalamus as a neuronal oscillator. Brain Research Rev. 8: 1-63

Steriade, M., Gloor, P., Llinas, R., Lopes da Silva, F., Mesulam, M. (1990). Basic mechanisms of cerebral rhythmic activities, Electroenceph. Clin. Neurophysiol. 76: 481-508.

Taylor, K., Mandon, S., Freiwald, W. A., Kreiter, A. K. (2005). Coherent oscillatory activity in monkey area V4 predicts successful allocation of attention. Brain Research Institute, Center for Emotional and Cognitive Cerebral Cortex. 5: 1424-1437.

Thorpe, S. J., Imbert, M., (1989). Biological constraints on connectionist models. In R. Pfeifer, Z. Schreter & F. Fogelman-Soulié, Connectionism in perspectice, Amsterdam Elservier. p. 63-92.

Thorpe, S., Delorme, A., Van Rullen, R. (2001). Spike based strategies for rapid processing, Neural Networks, 14(6-7): 715-726.

Turing, A. M. (1952). The Chemical Basis of Morphogenesis. Philosophical Transactions of the Royal Society of London. Series B, Biological Sciences, 237(641): 37-72.

Vreeken, J. (2003). Spiking neural networks, and introduction. Department of Information and Computing Sciences, Utrecht University.

Wang, X.J., Golomb, D., Rinzel, J. (1995). Emergent spindle oscillations and intermittent burst firing in a thalamic model: Specific neuronal mechanisms. Proc. Natl. Acad. Sci. 92(12): 5577-5581.

Wilson, H.R., Cowan, J.D. (1972). Excitatory and Inhibitory Interactions in Localized Populations of Model Neurons, Biophys. J. 12: 1-24.

Yakovlev, P. A., Lecours, I. R. (1967). The myelogenetic cycles of regional maturation of the brain. In A. Minkowski (Ed.), Regional development of the brain in early life. Oxford: Blackwell. p. 3-70.

Software

BRIAN v1.0.0rc4 available at: http://brian.di.ens.fr, accessed August 27, 2008.
NeuroSpec 2.0 available at: http://www.neurospec.org, accessed August 27, 2008.

Appendix

Python Neural Model Code

```
# Neuron and Neuron Network Model
# by Francis Jeanson 2008
# EASy MSc Thesis project
# Requires scipy, numpy, brian

from brian import *
import time
import random


###### Neuron Parameters

vr    = -90*mvolt    # Reset membrane potential
vt    = -55*mvolt    # Threshold
ref   =  1*msecond   # Refractory period

taue  =  10*msecond  # Somatic excitatory membrane time constant
taui  = 7.5*msecond  # Somatic inhibitory menmbrane time constant
taude =  2.*msecond  # Dendritic excitatory membrane time constant
taudi = 1.5*msecond  # Dendritic inhibitory membrane time constant
CV    = 0.05         # Coeficient of variation

tauge = 0.25*msecond # Excitatory conductance time constant
taugi = 0.75*msecond # Inhibitory conductance time constant

El    = -70*mvolt    # Resting potential
Ee    =   0*mvolt    # Reversal potential of excitatory ionic channels
Ei    = -80*mvolt    # Reversal potential of inhibitory ionic channels

tauI  = 0.1*msecond  # Currant flow time constant
gl    = 10.*nsiemens # Leak conductance
gld   =  5.*nsiemens # Leak conductance

# Compute the somatic and dendritic capacitance for each neuron type
Rmse = 600*Mohm # Excitatory cell membrane resistance
Rmsi = 800*Mohm # Inhibitory cell membrane resistance
Ces = taue/Rmse # Excitatory cell somatic capacitance
Ced = 3.*Ces    # Excitatory cell dendritic capacitance
Cis = taui/Rmsi # Inhibitory cell somatic capacitance
Cid = 3.*Cis    # Inhibitory cell dendritic capacitance
Rmde = 2.4*Rmse # Current flow resistance from excitatory dendrite to soma
Rmdi = 2.4*Rmsi # Current flow resistance from inhibitory dendrite to soma
```

```
###### Network Parameters

# Poisson input
Pinput = 1.0*nS  # Input weight
Pfreq  = 8.5*kHz # Input intensity

we = 0.5*nS # Excitatory synaptic weight
wi = 1.0*nS # Inhibitory synaptic weight

# Network sheet parameters
ePN = 2800 # Excitatory input width
iPN = 504  # Inhibitory input width
N  = 10000 # Total population number
eN = 8500  # Excitatory number
eNx = 100  # Excitatory x-axis dimension
eNy = 85   # Excitatory y-axis dimension
iN = 1500  # Inhibitory number
iNx = 50   # Inhibitory x-axis dimension
iNy = 30   # Inhibitory y-axis dimension

start_time=time.time()


###### Helpers

#Generate a list of Gaussians
def nvlist(mean, sd, leng, u):
    lst = []
    for i in range(0,leng):
        lst.append(random.gauss(mean,sd)*u)
    return qarray(lst)


###### Neuron Model

# Excitatory Neuron Equations
Eeqs=Equations('''
#Somatic Compartment
dv/dt  = (gl*(El-v)+ge*(Ee-v)+gi*(Ei-v)+Ids)/CesNV : volt
dge/dt = -ge/tauge : siemens
dgi/dt = -gi/taugi : siemens
CesNV = ((Ces/pF) + random.normalvariate(0,(Ces/pF)*CV))*pF : farad
```

```
#Dendritic Compartment
dvd/dt  = (gld*(El-vd)+ged*(Ee-vd)+gid*(Ei-vd))/CedNV : volt
dged/dt = -ged/tauge : siemens
dgid/dt = -gid/taugi : siemens
CedNV = ((Ced/pF) + random.normalvariate(0,(Ced/pF)*CV))*pF : farad

#Current from D to S
dIds/dt = (-Ids+((vd-v)/Rmde))/tauI : amp
''')

# Inhibitory Neuron Equations
Ieqs=Equations('''
#Somatic Compartment
dv/dt  = (gl*(El-v)+ge*(Ee-v)+gi*(Ei-v)+Ids)/CisNV : volt
dge/dt = -ge/tauge : siemens
dgi/dt = -gi/taugi : siemens
CisNV = ((Cis/pF) + random.normalvariate(0,(Cis/pF)*CV))*pF : farad

#Dendritic Compartment
dvd/dt  = (gld*(El-vd)+ged*(Ee-vd)+gid*(Ei-vd))/CidNV : volt
dged/dt = -ged/tauge : siemens
dgid/dt = -gid/taugi : siemens
CidNV = ((Cid/pF) + random.normalvariate(0,(Cid/pF)*CV))*pF : farad

#Current from D to S
dIds/dt = (-Ids+((vd-v)/Rmdi))/tauI : amp
''')


###### Neural Sheets

# Create Excitatory Neural Sheet
ENG  = NeuronGroup(eN,model=Eeqs,\
                   threshold=EmpiricalThreshold(threshold=vt,refractory=ref),\
                   implicit=True,freeze=True,compile=False, max_delay=8*ms)
ENG.v = nvlist(El/mV, 3, eN, mV) # Initialize voltage with noise
ENG.Ids = 0.0*amp*ones(eN)

# Create Inhibitory Neural Sheet
ING  = NeuronGroup(iN,model=Ieqs,\
                   threshold=EmpiricalThreshold(threshold=vt,refractory=ref),\
                   implicit=True,freeze=True,compile=False, max_delay=8*ms)
```

```
ING.v = nvlist(El/mV, 3, iN, mV) # Initialize voltage with noise
ING.Ids = 0.0*amp*ones(iN)

# Create Poisson input sheets
EPG  = PoissonGroup(ePN, rand(ePN)*Pfreq)
IPG  = PoissonGroup(iPN, rand(iPN)*Pfreq)

#status
print 'Created Neural Sheet', 'time:', time.time()-start_time, 'seconds'

# Connect Poisson input to excitatory neural sheet
ENGsub = ENG[(eN/2)-(ePN/2):(eN/2)-(ePN/2)+ePN] # Determine center of the sheet
EP = Connection(EPG,ENGsub,'ge')
EP.connect_one_to_one(EPG,ENGsub, weight=Pinput)

# Connect Poisson input to inhibitory neural sheet
INGsub = ING[(iN/2)-(iPN/2):(iN/2)-(iPN/2)+iPN] # Determine center of the sheet
IP = Connection(IPG,INGsub,'ge')
IP.connect_one_to_one(IPG,INGsub, weight=Pinput)

#status
print 'Connected Poisson Input', 'time:', time.time()-start_time, 'seconds'

# In the following:
# 0.05 because of 500 cells contacted by each excitatory cells from 10000 i.e.5%
# 0.13 probability of connection
# 1.66 inverse adjustment because range was 300um for each cell out of 500um,
# total suface 5/3 = 1.66
# The weight = lambda i,j expression is used to compute weight decay
# given source neuron i, and target j by distributing them on a two 2D grid.

# Connect excitatory to inhibitory
EICs = Connection(ENG, ING,'ge', delay=2*ms)
EICs.connect_random(ENG, ING, 0.05*0.13*1.66, \
weight=lambda i,j: exp(-abs(sqrt(pow((i/eNx)/float(eNx)-(j/iNx)/float(iNx),2) + \
pow((i%eNy)/float(eNy)-(j%iNy)/float(iNy),2))))*we)

EICd = Connection(ENG, ING,'ged', delay=2*ms)
EICd.connect_random(ENG, ING, 0.05*0.87*1.66, \
weight=lambda i,j: exp(-abs(sqrt(pow((i/eNx)/float(eNx)-(j/iNx)/float(iNx),2) + \
pow((i%eNy)/float(eNy)-(j%iNy)/float(iNy),2))))*we)
#status
print 'Connected Excit to Inhib', 'time:', time.time()-start_time, 'seconds'
```

```
# Connect excitatory to excitatory
EECd = Connection(ENG, ENG,'ged', delay=2*ms)
EECd.connect_random(ENG, ENG, 0.05*1.0*1.66, \
weight=lambda i,j: exp(-abs(sqrt(pow((i/eNx)/float(eNx)-(j/eNx)/float(eNx),2) + \
pow((i%eNy)/float(eNy)-(j%eNy)/float(eNy),2))))*we)
#status
print 'Connected Excit to Excit', 'time:', time.time()-start_time, 'seconds'


# Connect inhibitory to excitatory
IECs = Connection(ING, ENG,'gi', delay=6*ms)
IECs.connect_random(ING, ENG, 0.125*0.76*1.66, \
weight=lambda i,j: exp(-abs(sqrt(pow((i/iNx)/float(iNx)-(j/eNx)/float(eNx),2) + \
pow((i%iNy)/float(iNy)-(j%eNy)/float(eNy),2))))*wi)

IECd = Connection(ING, ENG,'gid', delay=6*ms)
IECd.connect_random(ING, ENG, 0.125*0.24*1.66, \
weight=lambda i,j: exp(-abs(sqrt(pow((i/iNx)/float(iNx)-(j/eNx)/float(eNx),2) +\
 pow((i%iNy)/float(iNy)-(j%eNy)/float(eNy),2))))*wi)
#status
print 'Connected Inhib to Excit', 'time:', time.time()-start_time, 'seconds'


# Connect inhibitory to excitatory
IICs = Connection(ING, ING,'gi', delay=6*ms)
IICs.connect_random(ING, ING, 0.125*0.77*1.66, \
weight=lambda i,j: exp(-abs(sqrt(pow((i/iNx)/float(iNx)-(j/iNx)/float(iNx),2) + \
pow((i%iNy)/float(iNy)-(j%iNy)/float(iNy),2))))*wi)

IICd = Connection(ING, ING,'gid', delay=6*ms)
IICd.connect_random(ING, ING, 0.125*0.23*1.66, \
weight=lambda i,j: exp(-abs(sqrt(pow((i/iNx)/float(iNx)-(j/iNx)/float(iNx),2) + \
pow((i%iNy)/float(iNy)-(j%iNy)/float(iNy),2))))*wi)
#status
print 'Connected Inhib to Inhib', 'time:', time.time()-start_time, 'seconds'


###### Prepare plotting resources

# Pick a neuron to record from randomly
nr = int(round(random.gauss(eN/2,eN/6)))
```

```
# Raster plot monitors
SpE = SpikeMonitor(ENG)
SpI = SpikeMonitor(ING)

# Generate spike time output files
FSpE = FileSpikeMonitor(ENG,'brian_EFSpM')
FSpI = FileSpikeMonitor(ING,'brian_IFSpM')

# Excitatory voltage state monitor
StM = StateMonitor(ENG,'v',record=[nr])

# Excitatory conductance monitor
SMe = StateMonitor(ENG, 'ged', record=[nr])

# Spike count monitors
Me  = PopulationSpikeCounter(ENG)
Mi  = PopulationSpikeCounter(ING)
SCe = SpikeCounter(ENG)

#status
print 'Created Monitors', 'time:', time.time()-start_time, 'seconds'



#status
print 'Running...'

###### Run the simulation
run(2*second)



###### Plot monitor output
print "Simulation time:",time.time()-start_time,"seconds"

# Print spike counts
print Me.nspikes+Mi.nspikes, '\ttotal spikes'
print Me.nspikes,  '\texcitatory spikes'
print Mi.nspikes,  '\tinhibitory spikes'

print SCe[nr], 'spikes for neuron', nr, 'in ENG'

subplot(221)
raster_plot(SpE)
ylabel('Excit Neuron Number')
```

```
subplot(222)
plot(SMe.times/ms, SMe[maxn]/nS)
xlabel('Time (ms)')
ylabel('Excit Conductance (mS)')

subplot(223)
raster_plot(SpI)
ylabel('Inhib Neuron Number')

subplot(224)
plot(StM.times/ms, StM[maxn]/mvolt)
xlabel('Time (ms)')
ylabel('Excit Potential (mV)')

show()
```

Matlab Analysis Code

```
%%%%%%%%%%%%%%%%%%
% pooled_spike_spectra.m
% This file computes the PSD from a pool of spike train
% data. This data is loaded from two files: r0X_EFSpM
% for the excitatory input, and from file: roX_IFSpM for
% inhibitory input.
% Requires the following functions:
% - get_histogram
clear;

%Unit
m = 10^-3;
Fs = 1/m;

mxt = [];
% Begin loop for pooled data collection
for g =1:5

    % Prepare input file names
    sp1name = strcat(strcat('r03.',int2str(g)), '_EFSpM');
    sp2name = strcat(strcat('r03.',int2str(g)), '_IFSpM');

    % Load files
    sp1 = load(sp1name);
    sp2 = load(sp2name);

    fp = [sp1;sp2];         %concatenate
    fp = sortrows(fp,2); %sort spike times
    sp = fp(:,2);              %store only times

    % Get histogram
    [hist, moment] = get_histogram(sp, 0.2);

    % Shuffle histogram: uncomment to test spectral saliency.
    %  shuf = zeros(1,length(hist));
    %  hist_tmp = zeros(1,length(hist));
    %  for i = 1:length(hist)
    %      in_shuf = 1;
    %      while in_shuf
    %          idx = round(rand(1)*length(hist));
    %          in_shuf = 0;
    %          for j = 1:length(shuf)
    %              if idx == shuf(j)
```

```
    %                   in_shuf = 1;
    %               end
    %           end
    %       end
    %       shuf(i) = idx;
    %       hist_tmp(i) = hist(idx);
    %   end
    %
    %   hist = hist_tmp;

    % The following code is adapted from the Matlab resource support code.
    % Use next highest power of 2 greater than or equal to length(x) to calculate FFT.
    nfft= 2^(nextpow2(length(hist)));
    % Take fft, padding with zeros so that length(fftx) is equal to nfft
    fftx = fft(hist,nfft);
    % Calculate the numberof unique points
    NumUniquePts = ceil((nfft+1)/2);
    % FFT is symmetric, throw away second half
    fftx = fftx(1:NumUniquePts);
    % Take the magnitude of fft of x and scale the fft so that it is not a
    % function of the length of x
    mx = abs(fftx)/length(hist);
    % Take the square of the magnitude of fft of x.
    mx = mx.^2;

    % Since we dropped half the FFT, we multiply mx by 2 to keep the same energy.
    % The DC component and Nyquist component, if it exists, are unique and should not
    % be mulitplied by 2.
    if rem(nfft, 2) % odd nfft excludes Nyquist point
      mx(2:end) = mx(2:end)*2;
    else
      mx(2:end -1) = mx(2:end -1)*2;
    end
    % This is an evenly spaced frequency vector with NumUniquePts points.
    f = (0:NumUniquePts-1)*Fs/nfft;

    % accumulate spectras
    mxt = [mxt;mx];
end

% Compute the averaged spectra
mx = sum(mxt)/size(mxt,1);
```

```
% Generate the plot, title and labels.
figure
plot(f,mx);
hold on;
plot(f, 3*std(mx(1,8:length(mx))), 'r-');
hold off;
title('Power Spectrum');
xlabel('Frequency (Hz)');
ylabel('Power');
```

```
%%%%%%%%%%%%%%%%%%
% pooled_lfp_coherence.m
% This file is used to compute the pooled spectra, phase
% coherence, and cumulant density of two distinct local
% field potentials.
% Requires the following functions:
% - lfp_ids
% - get_histogram
% - sp2a2_m1 (NeuroSpec 2.0)
% - psp2 (NeuroSpec 2.0)

% Sheet parameters
colnum = 50;  % number of neurons per column
rownum = 30; % number of neurons per row
fr     = 5;           % field radius

%Retrieve Local Field 1
a_x = round(rand(1)*(colnum-2*fr)+fr); % field x origin
a_y = round(rand(1)*(rownum-2*fr)+fr); % field y origin
a_x
a_y
%Retrieve Local Field 2
b_x = round(rand(1)*(colnum-2*fr)+fr); % field x origin
b_y = round(rand(1)*(rownum-2*fr)+fr); % field y origin
b_x
b_y



f_tot  = []; %frequency domain data store
t_tot  = []; %time domain data store
cl_tot = 0; %confidence limits data store

%Begin loop to pool data
iter = 5;
for g =1:iter

    fname = strcat(strcat('r02.',int2str(g)), '_IFSpM');
    fp = load(fname);

    %%% Create histogram of local field 1
    % Retrieve the neuron ids of the field
    neurids = lfp_ids(colnum, rownum, a_x-fr, a_y-fr, a_x+fr, a_y+fr);
    % Store spike times in sorted order for neurons in neurids only.
```

```
spktimes = [];
for i = 1:length(neurids)
    nid = neurids(i);
    spktimes = [spktimes; fp(find(fp(:,1)==nid,length(fp)),:)];
end
spktimes = sortrows(spktimes,2);
spktimes = spktimes(:,2); % remove neuron ids
% Get the potentials
[lfp1,moment1] = get_histogram(spktimes, 0.2);

%%% Create histogram of local field 2
% Retrieve the neuron ids of the field
neurids = lfp_ids(colnum, rownum, b_x-fr, b_y-fr, b_x+fr, b_y+fr);
% Store spike times in sorted order for neurons in neurids only.
spktimes = [];
for i = 1:length(neurids)
    nid = neurids(i);
    spktimes = [spktimes; fp(find(fp(:,1)==nid,length(fp)),:)];
end
spktimes = sortrows(spktimes,2);
spktimes = spktimes(:,2); % remove neuron ids
% Get the potentials
[lfp2,moment2] = get_histogram(spktimes, 0.2);

%%% Compute correlations of LFPs
% Pad the LFPs
diff = length(lfp1) - length(lfp2);
if length(lfp1) > length(lfp2)
    pad = zeros(1,diff);
    lfp2 = [lfp2,pad];
else
    pad = zeros(1,-diff);
    lfp1 = [lfp1,pad];
end

% Set mean = 0 and transpose
lfp1 = (lfp1-mean(lfp1))';
lfp2 = (lfp2-mean(lfp2))';

% For purposes of analysis: assume sampling rate is 1000/sec
samp_rate=1000;

% Set power for segment length as 9.
```

```
    % Thus T=2^9 = 512.
    % 512 points @ 1000/sec sampling gives segment length of 0.512 sec
    % Frequency resolution is inverse of this 1.953 Hz.
    seg_pwr=9;

    % Process these using sp2_m1
    opt_str='';  % Clear options

    % Process columns 1 and 2
    [f,t,cl]=sp2a2_m1(0,lfp1,lfp2,samp_rate,seg_pwr,opt_str);

    % sum the analysis
    if g == 1
        f_tot  = zeros(size(f));
        t_tot  = zeros(size(t));
    end

    f_tot  = f_tot+f;
    t_tot  = t_tot+t;
    cl_tot = cl_tot+cl.q_c95;
end

% average the data
f  = f_tot/iter;
t  = t_tot/iter;
cl.q_c95 = cl_tot/iter;

% plot the data
cl.what='LFP1 vs. LFP2';
figure
% The sampling rate defines the nyquist frequency as 500 Hz.
freq=150;     % Frequency To Display
lag_tot=500;
lag_neg=250;
ch_max=0.5;
psp2(f,t,cl,freq,lag_tot,lag_neg,ch_max)
```

```
%%%%%%%%%%%%%%%%%%
% get_histogram.m
% This file computes the histogram of an input spike time vector.

% Return the histogram of spike counts: hist
% and the time vector: moment.
% min_time the start time to record spike counts.
function [hist,moment] = get_histogram(spiketimes, mintime)

    sp = spiketimes;
    m = 10^-3;

    % Trim initial milliseconds
    fsp = [];
    for i=1:length(sp)
        if sp(i) >= mintime
            fsp(length(fsp)+1)=sp(i);
        end
    end
    sp = fsp;

    % Transform spike times to input signal i.e. spike count histogram
    % sp contains the times of spikes hence the number of records during
    % a window time is the number of spikes during that time.
    hist   = [];
    moment = [];
    if (length(sp)>0)
        window = 0.5*m;
        time = sp(1);
        index = 1;
        prev_length = 0;
        % Count the number of spike in the window over the entire sample set
        while time <= sp(length(sp))
            hist(index) = length(find(sp <= time+window)) - prev_length;
            prev_length = length(find(sp <= time+window));
            moment(index) = time;
            index = index + 1;
            time = time + window;
        end
    end
end
```

```
%%%%%%%%%%%%%%%%%%
% lfp.ids.m
% This file is used to retrieve the realistic 2D node ids.
% Returns the list of neurons in the field defined by
% A the sheet, tlx, the top left corner of the field,
% brx the bottom right corner of the field and their
% respective y positions.
function nids = lfp_ids(colnum, rownum, tlx, tly, brx, bry)
    nid = 1;
    nids = [];
    for i = 1:colnum
        for j = 1:rownum
            nid = ((i-1)*rownum)+j;
            if i>=tlx && i<brx && j>=tly && j<bry
                nids(length(nids)+1) = nid;
            end
        end
    end
end
```

```
%%%%%%%%%%%%%%%%%%
% coh_compare.m
% Plots the coherence difference between two LFP coherence vectors
% Requires that f_ext (coherence 1) and f (coherence 2) are
% in the memory space.

% store the x axis
x = [];
for i = 1:256
    x(i) = i/(length(f)/150);
end

% Plot the difference
figure
plot(x, f_ext(:,4)-f(:,4));
hold on;

% Plot the standard deviations
plot(x,-1.5*std(f_ext(:,4)-f(:,4))+mean(f_ext(:,4)-f(:,4)), 'b-');
plot(x,1.5*std(f_ext(:,4)-f(:,4))+mean(f_ext(:,4)-f(:,4)), 'b-');
plot(x,mean(f_ext(:,4)-f(:,4)), 'r-');

% Plot labels
xlabel('Frequency')
ylabel('Coherence Difference')
title('Coherence Comparison')
hold off
```